




Mathematical Analysis of Epidemic Models with Treatment in Heterogeneous Networks

Yi Wang^{1,2}  · Jinde Cao^{2,3} · Changfeng Xue⁴ · Li Li⁵

Received: 4 May 2022 / Accepted: 26 December 2022 / Published online: 5 January 2023

© The Author(s), under exclusive licence to Society for Mathematical Biology 2023

Abstract

In this paper, we formulate two different network-based epidemic models to investigate the effect of partly effective treatment on disease dynamics. The first network model represents the individuals with heterogeneous number of contacts in a population as choosing a new partner at each moment, whereas the second one assumes the individuals have fixed or stable neighbors. The basic reproduction number R_0 is computed for each model, using the next generation matrix method. In particular, the critical treatment rate is defined for the model, above which the disease can be eliminated through the treatment. The final epidemic size relations are derived, and the solvability of these implicit equations is studied. In particular, a unique solution of the implicit equation for the final epidemic size is determined, and by rewriting the implicit equation as a suitable fixed point problem, it is proved that the iteration of the fixed point problem converges to the unique solution. Stochastic simulations and numerical simulations, including in comparison with the model outputs and the joint influence of network topology and treatment on the final epidemic size, are conducted to illustrate the theoretical results.

✉ Yi Wang
wangyi-mail@163.com

Jinde Cao
jdciao@seu.edu.cn

Changfeng Xue
cfxue@163.com

Li Li
lili831113@sxu.edu.cn

¹ School of Mathematics and Physics, China University of Geosciences, Wuhan 430074, China

² School of Mathematics, Southeast University, Nanjing 210096, China

³ Yonsei Frontier Lab, Yonsei University, Seoul 03722, South Korea

⁴ School of Mathematics and Physics, Yancheng Institute of Technology, Yancheng 224051, China

⁵ School of Computer and Information Technology, Shanxi University, Taiyuan 030006, China

Keywords Treatment · Complex networks · Basic reproduction number · Final epidemic size · Solvability

1 Introduction

Emerging or reemerging infectious diseases have brought great threat to human population and public health. Recent identified diseases include, for example, pandemic of H1N1 influenza (2009) in Mexico, Middle East Respiratory Syndrome (2012) in Saudi Arabia and Corona Virus Disease 2019 (COVID-19) in China. The ongoing COVID-19 epidemic, first reported in Wuhan, China, on 31 December 2019, has caused the estimation of as much as 507, 184, 387 cumulative cases throughout the world, resulting in 6, 219, 657 deaths globally by 27 April 2022 (World Health Organization 2022). Therefore, it is crucial to design epidemiological surveys, collect necessary data, predict future trends, suggest control strategies and estimate forecast uncertainties (Hethcote 2000).

Generally speaking, it is very difficult or impossible to design epidemiological experiments with control in human population, hence, mathematical modeling in epidemiology provides a powerful tool to understand the potential mechanisms that affect the transmission of disease. Kermack and McKendrick (1927), two founders of modern mathematical epidemiology, established the general theory of classical infectious disease transmission models. Assuming the constant transmission and recovery rates, they obtained the classical susceptible–infectious–recovered (SIR) model as follows:

$$\begin{cases} S' = -\beta SI, \\ I' = \beta SI - \alpha I, \\ R' = \alpha I, \end{cases} \quad (1)$$

where $S(t)$, $I(t)$ and $R(t)$ represent the fraction or density of individuals who are susceptible to the disease, infectious having the ability to transmit the infection by contacts with susceptible individuals, and have got the infection and then recover from it at time t , respectively. Moreover, β is the transmission rate (i.e., the transmission probability times the contact rate that an individual can make per unit of time), α the recovery rate (i.e., $1/\alpha$ is the average infectious period for an infected individual), and the prime denotes the derivative with respect to time t (i.e., d/dt). Based on model (1), Kermack and McKendrick first established the threshold phenomenon of an epidemic, the so-called basic reproduction number R_0 nowadays, defined as the mean number of secondary cases caused by a typical infectious individual during its entire infectious period in a wholly susceptible population, and derived a final epidemic size relation, defined as the number or fraction of susceptible individuals who are infected at the end of an epidemic, to estimate the number of deaths for plague. Since then, lots of mathematical models are formulated to investigate the transmission and control of various infectious diseases (Anderson et al. 1992; Keeling and Rohani 2011; Sun et al. 2016).

In mathematical epidemic models, e.g., model (1), there are two important quantities frequently used to measure the severity of an epidemic. One is the basic reproduction number, and the other is the final epidemic size. Usually, the basic reproduction number R_0 determines the initial growth rate of an epidemic, the local asymptotic stability of disease-free equilibrium (van den Driessche and Watmough 2002) or the threshold condition that a disease could invade a population; the final epidemic size determines the attack rate of a disease under consideration. In recent years, basic reproduction number and final epidemic size have been widely studied deviating from the classical SIR model (1). For example, motivated by the idea of the basic reproduction number for disease models in homogeneous populations, Diekmann et al. (1990) gave the definition and the computation of the basic reproduction number R_0 for disease models in heterogeneous populations. Bacaër and Guernaoui (2006) established a generalization of the definition of the basic reproduction number in periodic environments. Later, Wang and Zhao (2008) presented the basic reproduction number and its computation formulae for a large class of periodic compartmental epidemic models, which determines the local stability of the disease-free periodic solution and even the global dynamics under certain circumstances. Diekmann et al. (2010) presented a detailed easy construction method for the next-generation matrices of compartmental epidemic models, which can describe the characteristic of the basic reproduction number. Ma and Earn (2006) extended the well-known final size relation to more complicated models by including a latent stage, arbitrary number of distinct infectious stages or a general class of spatial contact structures. Arino et al. (2007) obtained a final size relation for a general class of epidemic models, including the model with multiple susceptible classes. Later, Brauer (2017) adapted the approach to diseases transmitted through both a vector and a possibility of direct transmission. Magal and Webb (2018) proposed a method of identifying model parameters for SIR epidemics based upon the well-known final size relation.

It should be stressed that one key assumption of the model (1) analysis and its variants is that the individuals of a population are homogeneously mixed. Due to this assumption, classical epidemic models are usually called scalar deterministic models. This assumption is certainly too simple, and it has been recognized that if this assumption is violated then the well-known final size relation may not hold. In particular, the existence of super-spreaders, making many contacts and being instrumental in sexually transmitted diseases, leads to a different relation for the final size. To be more realistic and include heterogeneous mixing of a population, Brauer (2008) analyzed a two-group SIR epidemic model with treatment and derived the final size relation, which includes arbitrary mixing between the two groups. Recently, Magal et al. (2016) considered a two-group SIR epidemic model, investigated the final epidemic size for each group, and analyzed the qualitative behavior of the infectious classes at the early stage of the epidemic. Furthermore, final size relation of a multi-group SIR epidemic model (Magal et al. 2018) including irreducible and non-irreducible modes of transmission was investigated, the asymptotic behavior of the solutions for the implicit final size equations was analyzed in detail, and a computational algorithm for the final epidemic size was provided. To consider the heterogeneous mixing of a host population, a natural and more general approach is to use complex network models (Newman 2010), which can describe the characteristics of real-world systems more accurately. In net-

work terminology, each node represents an individual, and each edge denotes possible contacts between its two nodes; these two nodes are called neighbors of each other. Thus, the network defined constitutes a substrate over which the infectious disease spreads. Various network disease models have been formulated in the literature. For example, Moreno et al. (2002) obtained the epidemic threshold and estimated the final epidemic size for the SIR model in networks with different degree distributions. Zhang and Jin formulated a susceptible-exposed-asymptotically infected-symptomatically infected-recovered (SEAIR) epidemic model in heterogeneous networks (Zhang and Jin 2010) or with community structure (Zhang and Jin 2012), and derived the final size equations for these network epidemic models. Cao et al. (2015) studied an epidemic model with carrier state and birth and death events in heterogeneous networks, and presented the final size equations if birth and death events were ignored. Zhang et al. (2019) proposed a two-strain pairwise SIR epidemic model with non-Markovian recovery process, and obtained lower and upper bounds on the final epidemic size.

Although various types of network disease models have been formulated in the literature, one key distinguishing feature of these models is whether the network and the epidemic process evolve at different paces or time-scales (Zino and Cao 2021). In particular, if the network and the epidemic process evolve at the same paces, then the network co-evolves with and is influenced by the spread of the disease; if the network and the epidemic process evolve at different paces, then time-scale separation techniques are often used to deal with epidemics on dynamic networks. In the latter case, two extreme scenarios appear: annealed and quenched network models. These two types of network models are of great research value, shedding some light on the impact of network topology on disease dynamics. For example, the influential work on the continuous-time SIS model in annealed networks is Pastor-Satorras and Vespignani (2001). This work introduces a dynamical model for the spread of virus infections in scale-free networks, finding the absence of an epidemic threshold if the secondary moment of the degree distribution is diverging and its associated critical behavior. This article provides an unexpected result that changes radically lots of standard conclusions on epidemic spreading, that is, infections can proliferate on some types of scale-free networks no matter what transmission rates they may have. Following the pioneering network of Pastor-Satorras and Vespignani (2001), there have been many studies on the mathematical modeling of disease spread in annealed networks (Kiss et al. 2006; Wang and Dai 2008; Wang et al. 2012; Sanz et al. 2014; Gupta et al. 2021). We notice that most of these studies focus on the calculation of the basic reproduction number or epidemic threshold, the final epidemic size or stationary density of infected individuals and the dynamical analysis (e.g., local or global stability of the equilibria) of the model.

Levin and Durrett (1996) argue that the individual-level dynamics of infectious diseases may involve higher-order correlations. Following this idea, Keeling et al. (1997) proposed pairwise models for childhood diseases, attempting to capture the underlying correlations between individuals. Since then, various mathematical models on epidemic spreading in quenched networks have been formulated (Keeling 1999; Newman 2002; Eames and Keeling 2002; Lindquist et al. 2011; Corcoran and Hastings 2021). We find that most of these works focus on the calculation of the basic reproduction number or epidemic threshold, the final epidemic size and comparing

model outputs with stochastic epidemic simulations. Because most of these models are high-dimensional and strong nonlinear, it is often very difficult to obtain analytical results, but an exception is Corcoran and Hastings (2021), in which asymptotic techniques are used to derive an approximation for the endemic equilibrium when it exists. Moreover, individual-based or agent-based models are proposed to describe the dynamic behavior of epidemic processes over networks (Paré et al. 2020).

Among the studies on network epidemic models mentioned above, we notice that although the final size equations or relations are derived for homogeneously or heterogeneously mixed population, the solvability of implicit equations for final epidemic size are not well understood, and they have been less studied. In Bidari et al. (2016), Bidari et al. studied the solvability of implicit equations for the final epidemic size such as the classical SIR model, the pairwise SIR model and the heterogeneous mean-field SIR model, and proved the convergence of the solution for a suitable fixed point equation. Wang and Cao (2021) studied the final size of various network SIR models, and showed that how the final epidemic size is related to the basic reproduction number for different degree distributions.

On the other hand, treatment is the care provided to reduce morbidity and mortality of an infectious diseases, and it is one of the most important measures to relieve the spread of the disease (Wang 2006). One form of treatment that may be available for some diseases is vaccine to protect against infection before the initiation of a disease. In particular, as early as the 18th century, Daniel Bernoulli formulated a mathematical model for smallpox to evaluate the effectiveness of variolation of healthy people (Hethcote 2000). The essential of treatment is to cure or mitigate a disease through the use of an agent, procedure, or regimen, including a drug, or bed rest. This measure is effective for most infectious diseases, such as malaria, tuberculosis, and COVID-19. Epidemic models with treatment have been widely studied in the literature. For instance, Feng et al. (2000) formulated a model for tuberculosis with exogenous reinfection where a proportion of treated people may acquire new infection from other infectious individuals, and showed that the model can have multiple endemic equilibria even for $R_0 < 1$. Wang and Ruan (2004) proposed an epidemic model with constant removal rate of infectious individuals to evaluate the effect of limited resources for treatment of infectives on the disease spread, and showed that the model can undergo several types of bifurcations. Yan and Wang (2019) studied the impact of shock-kill strategy where broadly neutralizing antibodies (bNAbs) are injected with a combination of HIV latency activators on the treatment of HIV dynamics. In reality, treatment is not always completely effective, decreasing the rate of infection and also decreasing infectivity if a treated individual does become infected. Thus, a treated individual may have a lower rate of infection and also infectivity. The following system of ordinary differential equations (ODEs) for infectious diseases with treatment is taken from Brauer and Castillo-Chavez (2012) but with the fraction instead of the number of individuals:

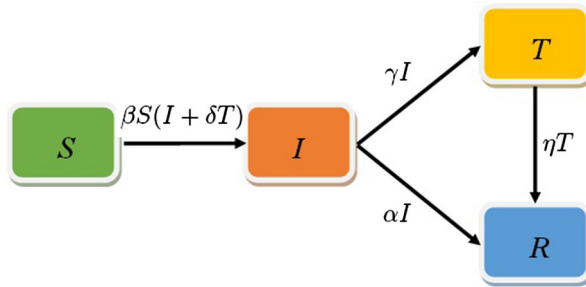


Fig. 1 Flow diagram for the homogeneous mixing SITR model. The transition rates between different compartments are marked on the arrows. (Online version in color)

$$\begin{cases} S' = -\beta S(I + \delta T), \\ I' = \beta S(I + \delta T) - (\alpha + \gamma)I, \\ T' = \gamma I - \eta T, \\ R' = \alpha I + \eta T, \end{cases} \quad (2)$$

in which the treatment for infected individuals is assumed to be proportional to the fraction of infected individuals. This assumption is reasonable when medical resources are adequate, or when the disease under consideration is non-fatal. Once a individual has been infected, a fraction γ of infected individuals is chosen to be treated. Moreover, treated individuals have reduced infectivity by a factor δ ($0 \leq \delta \leq 1$); alternatively, $1 - \delta$ measures the effectiveness of treatment. The parameter $1/\eta$ denotes the average treatment period for an treated individual to recover (the treated individual is more easily to recover, i.e., $\eta > \alpha$), and other parameters are the same as in model (1). The flowchart with marked transition rates is depicted in Fig. 1.

Based on the above discussions, in this paper, we will focus on the mixing patterns of groups of individuals of the host population through complex network models. In particular, we propose two different network-based SITR models with the assumption of adequate medical resources, that is, the capacity of treatment for infected individuals is linearly correlated with the density or number of infected individuals. One is based on the annealed network model, which is essentially a multi-group epidemic model, and can be seen as an extension to the two-group SITR model (similar to model (2)) with preferred mixing in Brauer (2008). The other is based on the quenched network models, which can account for the status correlations between individuals due to the ‘consumption’ of susceptible individuals/nodes in the neighborhood. For these models, we derive the final size equations, and prove that those implicit equations for the final epidemic size have unique solutions for an arbitrary degree distribution. Furthermore, by rewriting the implicit equation as a suitable fixed point equation, a computational algorithm that is shown to be stable is developed for estimating the final epidemic size.

The rest of the paper is organized as follows. In Sect. 2, we formulate an epidemic model with treatment in annealed networks with degree correlation, derive the final size equations, and prove the solvability of implicit equations for the final epidemic

size. Specifically, for annealed networks with no degree correlation, we give a low-dimensional equivalent system and an explicit expression of the basic reproduction number. In Sect. 3, we formulate a low-dimensional epidemic model with treatment in quenched networks, compare the model output with stochastic simulations for Poisson and scale-free degree distributions, obtain the final size equation, and prove the solvability of the associated implicit equation. In Sect. 4, we give a brief summary and the discussion of our article.

2 Epidemic Models with Treatment in Annealed Networks

Annealed network models mean that the network dynamics evolves much faster than the dynamical processes such as the spread of a pathogen or the diffusion of a product in them. In other words, the nodes of a network are constantly rewired. In particular, for the spread of a disease in annealed networks, the spread of an infection is possible only if a ‘stub’ of an infectious node is connected to a ‘stub’ of a susceptible node. Usually, the dynamical process in annealed networks can be well captured by the so called heterogeneous mean-field (HMF) theory (Pastor-Satorras et al. 2015); that is, nodes with the same degree are considered to be statistically equivalent.

2.1 Heterogeneous Mean-Field (HMF) Epidemic Model with Treatment

To incorporate heterogeneity in the contacts among individuals of a population, we first classify individuals by their number of contacts. Assume that the population is classified as n distinct groups of sizes N_k ($k = 1, \dots, n$), where n is the maximum number of contacts that an individual can have. Then, the total population size is $N = \sum_{i=1}^n N_k$, and the probability that a randomly chosen individual has the number of k contacts is $P(k) = N_k/N$, which is called degree distribution in network terminology. Furthermore, the individuals in group k are classified by their infection statuses. Let $S_k(t)$, $I_k(t)$, $T_k(t)$ and $R_k(t)$ be the relative density (where the number of degree k nodes in each state is divided by N_k) of susceptible, infected, treated and recovered individuals with degree k at time t , respectively. Based on the heterogeneous mean-field theory, we extend the homogeneous model (2) to annealed network models and obtain the following system of ordinary differential equations:

$$\begin{cases} S'_k = -\tau k S_k \Theta_k^I - \delta \tau k S_k \Theta_k^T, \\ I'_k = \tau k S_k \Theta_k^I + \delta \tau k S_k \Theta_k^T - (\alpha + \gamma) I_k, \\ T'_k = \gamma I_k - \eta T_k, \\ R'_k = \alpha I_k + \eta T_k, \end{cases} \quad (3)$$

where the prime represents the derivative of a state variable with respect to time t , τ is the transmission rate across a network contact between an infected node and a susceptible one, and parameters δ , α , γ and η are defined above as model (2). The quantities $\Theta_k^I = \sum_l P(l|k) I_l(t)$ and $\Theta_k^T = \sum_l P(l|k) T_l(t)$ are the probabilities that a node of degree k connects to infected and treated nodes of arbitrary degree l at

time t , respectively, where $P(l|k)$ denotes the conditional probability that a node of degree k connects to a node of degree l , and satisfies the normalization condition $\sum_l P(l|k) = 1$.

The initial conditions for model (3) are

$$S_k(0) = 1 - \epsilon_k \geq 0, \quad I_k(0) = \epsilon_k \geq 0, \quad T_k(0) = R_k(0) = 0.$$

It is reasonable to assume that there are no treated and recovered individuals in the population initially, especially when a new disease appears.

Since the state variable R_k does not appear in the first three equations of model (3), using the normalization condition $S_k(t) + I_k(t) + T_k(t) + R_k(t) = 1$, we obtain a simplified system. Denote

$$\Gamma = \{(S_1, I_1, T_1, \dots, S_n, I_n, T_n) \in \mathbb{R}_+^{3n} | S_k, I_k, T_k \geq 0, S_k + I_k + T_k \leq 1\},$$

with $k = 1, \dots, n$, and n is the maximum degree allowed due to the finite network size effect (Pastor-Satorras and Vespignani 2002; Wang and Cao 2014). The following preliminary result shows that the model (3) is epidemiologically and mathematically well-posed.

Lemma 2.1 *System (3) admits a unique solution that exists for all $t \geq 0$ with initial condition starting from Γ . Moreover, the compact set Γ is positively invariant with respect to system (3).*

Proof It is easy to show that the vector field determined by the right-hand sides of (3) is locally Lipschitz continuous in Γ , so there exists a unique solution of system (3) for all $t \geq 0$.

The nonnegative property of state variables can be directly verified according to the associated model equations. For example, rewriting the first equation of (3) as $(\ln S_k)' = -\tau k \Theta_k^I - \delta \tau k \Theta_k^T$ and integrating it from 0 to t , we have

$$S_k(t) = S_k(0) e^{-\tau k \int_0^t (\Theta_k^I(s) + \delta \Theta_k^T(s)) ds} \geq 0,$$

for any $t \geq 0$. Similarly, integrating the second equation of (3) yields

$$I_k(t) = I_k(0) e^{-(\alpha + \gamma)t} + \tau k e^{-(\alpha + \gamma)t} \int_0^t S_k(s) (\Theta_k^I(s) + \delta \Theta_k^T(s)) e^{(\alpha + \gamma)s} ds.$$

From the above expression, it suffices to show $\Theta_k^I(t) \geq 0$ and $\Theta_k^T(t) \geq 0$ for all $t \geq 0$ and $1 \leq k \leq n$. To see this, multiplying the second and third equation of (3) by $P(l|k)$ and summing over l , respectively, we obtain

$$\begin{cases} \frac{d\Theta_k^I}{dt} = \tau \sum_{l=1}^n l S_l P(l|k) (\Theta_k^I + \delta \Theta_k^T) - (\alpha + \gamma) \Theta_k^I, \\ \frac{d\Theta_k^T}{dt} = \alpha \Theta_k^I - \eta \Theta_k^T, \quad k = 1, \dots, n. \end{cases}$$

For a fixed k , notice that the above system is homogeneous linear with respect to Θ_k^I and Θ_k^T . If $\Theta_k^I = 0$, then $d\Theta_k^I/dt \geq 0$. Similar argument applies to Θ_k^T . If $\Theta_k^I + \Theta_k^T = 1$, i.e., $S_l = 0$ for all $1 \leq l \leq n$, then $d(\Theta_k^I + \Theta_k^T)/dt = -\gamma\Theta_k^I - \eta\Theta_k^T \leq 0$. It follows that $0 \leq \Theta_k^I(t) \leq 1$ and $0 \leq \Theta_k^T(t) \leq 1$ for all $1 \leq k \leq n$. Hence, it follows that $I_k(t) \geq 0$, for $t \geq 0$ and $k = 1, \dots, n$.

Integrating the third equation of (3) gives

$$T_k(t) = T_k(0)e^{-\eta t} + \gamma e^{-\eta t} \int_0^t I_k(s)e^{\eta s} ds \geq 0, \quad k = 1, \dots, n, \text{ and } t \geq 0.$$

Finally, the total population over the same degree k satisfies $n'_k = (S_k + I_k + T_k + R_k)' = 0$, which implies $S_k(t) + I_k(t) + T_k(t)$ is bounded above by one for all $t \geq 0$. \square

For the long-time behavior of solutions for model (3), the following lemma holds, which shows the disease will burn out at last.

Lemma 2.2 *For system (3), it holds that*

$$S_k(+\infty) = \lim_{t \rightarrow +\infty} S_k(t) \geq 0, \quad \lim_{t \rightarrow +\infty} I_k(t) = \lim_{t \rightarrow +\infty} T_k(t) = 0, \quad k = 1, \dots, n.$$

Proof From Lemma 2.1, it is obvious that $S'_k(t) \leq 0$ for all $t \geq 0$. Since $S_k(t) \geq 0$, the limit $S_k(+\infty) \geq 0$, $k = 1, \dots, n$, exists. Similar argument applies to $S_k(t) + I_k(t)$ (noting that $(S_k + I_k)' = -(\alpha + \gamma)I_k$). It follows that the limit $I_k(+\infty) \geq 0$, $k = 1, \dots, n$, exists. If $\lim_{t \rightarrow +\infty} I_k(t) = \iota > 0$, then $I_k(t) > \iota/2$ for sufficiently large t . On the other hand, integrating the equation of $(S_k + I_k)'$ and taking a limit $t \rightarrow +\infty$, we have

$$1 - S_k(+\infty) - \iota = (\alpha + \gamma) \int_0^{+\infty} I_k(s) ds \geq \frac{(\alpha + \gamma)\iota}{2} t \Big|_0^{+\infty} \rightarrow +\infty,$$

which contradicts with the boundedness of $S_k(+\infty)$. Hence, we conclude $I_k(+\infty) = \lim_{t \rightarrow +\infty} I_k(t) = 0$.

Noting that $(S_k + I_k + T_k)' = -\alpha I_k - \eta T_k$. Similar to our analysis of the existence of limit of $I_k(+\infty)$, it is easy to verify that $T_k(+\infty) = \lim_{t \rightarrow +\infty} T_k(t) = 0$. Moreover, it immediately follows that $R_k(+\infty)$ exists and that $R_k(+\infty) = 1 - S_k(+\infty)$, $k = 1, \dots, n$. \square

2.2 Basic Reproduction Number and Final Size Equations

In this subsection, we first calculate the basic reproduction number R_0 and define a critical treatment rate above which the disease can be eliminated. Then we derive the final size equations of a disease. At the end we analyze the existence, uniqueness and solvability of the solution of the implicit equations for final epidemic size.

To calculate the basic reproduction number R_0 for model (3), we order the infectious compartments first by disease status, then by degree, i.e.,

$$I_1, I_2, \dots, I_n, T_1, T_2, \dots, T_n.$$

Following the next generation matrix method of van den Driessche and Watmough (2002) we obtain the new infection matrix F and the transition matrix V , respectively, that is,

$$F = \begin{bmatrix} A_{11} & A_{12} \\ 0 & 0 \end{bmatrix} \text{ and } V = \begin{bmatrix} (\alpha + \gamma)E_n & 0 \\ -\gamma E_n & \eta E_n \end{bmatrix},$$

where $A_{11} = (\tau k P(l|k))_{n \times n}$, $A_{12} = (\delta \tau k P(l|k))_{n \times n}$, and E_n is the unit matrix of n th-order.

Then, the basic reproduction number R_0 of model (3) is the spectral radius of the matrix FV^{-1} , i.e., $R_0 = \rho(FV^{-1})$, where $\rho(\cdot)$ signifies the spectral radius of a square matrix, and

$$FV^{-1} = \begin{bmatrix} \frac{1}{\alpha + \gamma} A_{11} + \frac{\gamma}{(\alpha + \gamma)\eta} A_{12} & \frac{1}{\eta} A_{12} \\ 0 & 0 \end{bmatrix}.$$

The last n rows of FV^{-1} are zero, thus the spectral radius of this matrix is computed as

$$R_0 = \rho\left(\frac{1}{\alpha + \gamma} A_{11} + \frac{\gamma}{(\alpha + \gamma)\eta} A_{12}\right) = \left(\frac{\tau}{\alpha + \gamma} + \frac{\gamma}{\alpha + \gamma} \frac{\delta \tau}{\eta}\right) \rho(A), \quad (4)$$

where $A = (kP(l|k))_{n \times n}$. Note that R_0 is dependent on all model parameters and network parameters that is encapsulated in $\rho(A)$. Moreover, R_0 is the sum of R_I and R_T , where $R_I = \tau \rho(A)/(\alpha + \gamma)$ and $R_T = \gamma \delta \tau \rho(A)/((\alpha + \gamma)\eta)$ are the number of secondary cases produced by an infected and treated individual while entering a wholly susceptible population, respectively.

Epidemiologically, $R_0 = 1$ is a disease threshold. In particular, if $R_0 < 1$, there will be no epidemic, whereas if $R_0 > 1$, there will be an outbreak without considering the stochasticity. The threshold condition $R_0 > 1$ is equivalent to

$$\rho(A) > \frac{(\alpha + \gamma)\eta}{(\eta + \delta \gamma)\tau},$$

which means that the connectivity matrix A encapsulating network topology information can have a great impact on the spread of the disease.

If $\gamma = 0$ and $\eta \rightarrow +\infty$, we retrieve the SIR model in annealed networks (Moreno et al. 2002). The basic reproduction number R_0 of SIR epidemic in annealed networks is $R_0 = \tau \rho(A)/\alpha$. If $\gamma > 0$, that is, once a node becomes infected a treatment is started, the basic reproduction number R_0 in (4) is usually called the control reproduction

number, customarily denoted as R_0^c . Computing the derivative of R_0^c with respect to γ yields

$$\frac{\partial R_0^c}{\partial \gamma} = \frac{\tau(\delta \frac{\alpha}{\eta} - 1)}{(\alpha + \gamma)^2} \rho(A).$$

It is worth noting that if $\delta = 0$, $\partial R_0^c / \partial \gamma < 0$, that is, increasing the treatment rate γ results in R_0^c decreasing and thus is beneficial to disease control, and if $0 < \delta \leq 1$, the fact $\eta > \alpha$ yields $\partial R_0^c / \partial \gamma < 0$, that is, R_0^c is decreasing with respect to γ . Thus, there must exist a critical treatment rate

$$\gamma^* = \frac{\frac{\tau \rho(A)}{\alpha} - 1}{1 - \frac{\delta \tau}{\eta} \rho(A)},$$

such that the disease can be eliminated from the network if $\gamma > \gamma^*$, $\frac{\tau \rho(A)}{\alpha} > 1$ (i.e., the disease spreads out without the treatment) and $\frac{\delta \tau}{\eta} \rho(A) < 1$ (i.e., the disease cannot spread out with the transmission of treated individuals alone).

In order to give more insight into the expression for R_0 , it is necessary to make some assumption on the nature of the mixing among different degree classes. One extreme case is degree uncorrelated, that is, the probability that a ‘stub’ links to nodes of degree l is proportional to the total ‘stubs’ they have, i.e., $P(l|k) = lP(l)/\langle k \rangle$, where $\langle k \rangle = \sum_l lP(l)$ is the mean degree of a network. Then, it is easy to obtain $\rho(A) = \langle k^2 \rangle / \langle k \rangle$, where $\langle k^2 \rangle = \sum_l l^2 P(l)$ is the second moment of the degree distribution. It follows from (4) that

$$R_0 = \left(\frac{\tau}{\alpha + \gamma} + \frac{\gamma}{\alpha + \gamma} \frac{\delta \tau}{\eta} \right) \frac{\langle k^2 \rangle}{\langle k \rangle}.$$

Remark 2.3 In Brauer (2008), Brauer extended the model (2) to a two-group epidemic model with different activity levels, i.e., τ_i , α_i and η_i ($i = 1, 2$) in our notation. The parameter p_{ij} ($i, j = 1, 2$) in Brauer (2008), defined as the fraction of contacts made by a member of group i that is with a member of group j , corresponds to the conditional probability $P(j|i)$ in our model (3). However, our model is more general than that in Brauer (2008), and describes arbitrary heterogeneity in mixing pattern of a population. In particular, consider the proportionate mixing as in Brauer (2008), i.e., $p_{ij} = a_j N_j / (a_1 N_1 + a_2 N_2)$, where a_i is the number of contacts that group i members make in unit time, one obtains the basic reproduction number for uncorrelated networks with bimodal degree distribution.

In the following, we establish the final epidemic size equations for the model (3). Let $\beta_{kl} = kP(l|k)$, then we can rewrite the first equation of (3) as

$$S'_k = -\tau S_k \sum_{l=1}^n \beta_{kl} I_l - \delta \tau S_k \sum_{l=1}^n \beta_{kl} T_l, \quad (5)$$

or equivalently

$$\frac{d \ln S_k}{dt} = -\tau \sum_{l=1}^n \beta_{kl} I_l - \delta \tau \sum_{l=1}^n \beta_{kl} T_l. \quad (6)$$

Integrating Eq. (6) from 0 to t gives

$$\ln S_k(t) - \ln(1 - \epsilon_k) = -\tau \sum_{l=1}^n \beta_{kl} \int_0^t I_l(s) ds - \delta \tau \sum_{l=1}^n \beta_{kl} \int_0^t T_l(s) ds. \quad (7)$$

Summing the first two equations of (3) leads to

$$\frac{d(S_k + I_k)}{dt} = -(\alpha + \gamma) I_k,$$

and then integrating it from 0 to t gives

$$S_k(t) + I_k(t) - 1 = -(\alpha + \gamma) \int_0^t I_k(s) ds, \quad t > 0. \quad (8)$$

Similarly, summing the first three equations of (3) yields

$$\frac{d(S_k + I_k + T_k)}{dt} = -\alpha I_k - \eta T_k,$$

and then integrating it from 0 to t gives

$$S_k(t) + I_k(t) + T_k(t) - 1 = -\alpha \int_0^t I_k(s) ds - \eta \int_0^t T_k(s) ds, \quad t > 0. \quad (9)$$

Hence, from Eq. (8) we have

$$\int_0^t I_k(s) ds = \frac{1}{\alpha + \gamma} - \frac{1}{\alpha + \gamma} (S_k(t) + I_k(t)). \quad (10)$$

Plugging Eq. (10) into Eq. (9), we have

$$\int_0^t T_k(s) ds = \frac{1}{\eta} - \frac{1}{\eta} (S_k(t) + I_k(t) + T_k(t)) - \frac{\alpha}{\eta(\alpha + \gamma)} (1 - S_k(t) - I_k(t)). \quad (11)$$

Inserting Eqs. (10) and (11) into Eq. (7), we obtain

$$\frac{\tau(\eta + \delta\gamma)}{\eta(\alpha + \gamma)} \sum_{l=1}^n \beta_{kl} (1 - S_l(t) - I_l(t)) - \frac{\delta\tau}{\eta} \sum_{l=1}^n \beta_{kl} T_l(t) + \ln S_k(t) = \ln(1 - \epsilon_k). \quad (12)$$

Observing that Eq. (12) holds for any $t > 0$, we conclude the following conservation equation:

$$\frac{d}{dt} \left\{ \frac{\tau(\eta + \delta\gamma)}{\eta(\alpha + \gamma)} \sum_{l=1}^n \beta_{kl}(1 - S_l(t) - I_l(t)) - \frac{\delta\tau}{\eta} \sum_{l=1}^n \beta_{kl}T_l(t) + \ln S_k(t) \right\} \equiv 0, \quad \forall t > 0,$$

$k = 1, \dots, n$. Integrating it from 0 to $+\infty$ and using Lemma 2.2, we have

$$\ln S_k(+\infty) = \frac{\tau(\eta + \delta\gamma)}{\eta(\alpha + \gamma)} \sum_{l=1}^n \beta_{kl}(S_l(+\infty) - 1) + \ln(1 - \epsilon_k).$$

More precisely, the final size equations are given by the following system:

$$\begin{cases} S_1(+\infty) = (1 - \epsilon_1) \exp \left\{ \frac{\tau(\eta + \delta\gamma)}{\eta(\alpha + \gamma)} \sum_{l=1}^n \beta_{1l}(S_l(+\infty) - 1) \right\}, \\ \vdots \\ S_n(+\infty) = (1 - \epsilon_n) \exp \left\{ \frac{\tau(\eta + \delta\gamma)}{\eta(\alpha + \gamma)} \sum_{l=1}^n \beta_{nl}(S_l(+\infty) - 1) \right\}. \end{cases} \quad (13)$$

Remark 2.4 Although Eq. (13) does not involve the basic reproduction number R_0 explicitly, it is still possible to estimate the final size of the disease from the model parameters. For the case of proportionate mixing, corresponding to our model (3) with bimodal degree distribution, Brauer (2008) obtained simple final size relations, and found that the final size relation can be expressed as in terms of the components of R_0 . It is impossible to obtain a simple final size relation for our model (3) with general degree distribution, however, for specific degree distribution, we may obtain simple final size relation involving R_0 explicitly as in Wang and Cao (2021).

To show that the implicit Eq. (13) for the final epidemic size admits a unique set of final density of susceptible nodes in each degree k , we introduce the map: $G : R^n \rightarrow R^n$ as

$$G(X) = (G_1(X), \dots, G_n(X))^T, \quad X \in R^n,$$

where A^T represents the transpose of a vector or matrix A , and

$$G_k(X) = (1 - \epsilon_k) \exp \left\{ \frac{\tau(\eta + \delta\gamma)}{\eta(\alpha + \gamma)} \sum_{l=1}^n \beta_{kl}(X_l - 1) \right\}, \quad k = 1, \dots, n.$$

To show the existence and uniqueness of the solution of (13), the following notations are useful. For any $X, Y \in R^n$, $X_l \leq Y_l$, for $l = 1, \dots, n \Leftrightarrow X \leq Y$; $X \leq Y$ and $X_l < Y_l$, for some $l = 1, \dots, n \Leftrightarrow X < Y$; $X_l < Y_l$, for $l = 1, \dots, n \Leftrightarrow X \ll Y$.

It is easy to see that G is monotone increasing, which means that if $X \leq Y$, then $G(X) \leq G(Y)$. In particular, if $0 \leq \epsilon_k < 1$, $k = 1, \dots, n$, i.e., $S_k(0) > 0$ and $I_k(0) \geq 0$, it follows that

$$0 \ll G(0) \leq G(\xi) \leq \xi,$$

where $\xi = (S_1(0), \dots, S_n(0))^T = (1 - \epsilon_1, \dots, 1 - \epsilon_n)^T$.

Furthermore, using the method of mathematical induction, we deduce that for each $j \geq 1$, it holds that

$$0 \ll G(0) \leq \dots \leq G^j(0) \leq G^{j+1}(0) \leq G^{j+1}(\xi) \leq \dots \leq G(\xi) \leq \xi.$$

According to the criterion of monotone bounded sequence, letting $j \rightarrow +\infty$ gives

$$0 \ll \lim_{j \rightarrow +\infty} G^j(0) \doteq \xi^- \leq \xi^+ \doteq \lim_{j \rightarrow +\infty} G^j(\xi) \leq \xi.$$

Since G is continuous, we conclude that $0 \ll G(\xi^-) = \xi^-$, $G(\xi^+) = \xi^+$, leading to the following result.

Lemma 2.5 *Assume that $\alpha + \gamma > 0$, $\eta > 0$ and $0 \leq \epsilon_k < 1$, $k = 1, \dots, n$. Then, the interval $[\xi^-, \xi^+]$ contains all the fixed points of G in $[0, \xi]$.*

Since G is continuously differentiable, for $k, l = 1, \dots, n$, we have

$$\frac{\partial G_k(X)}{\partial X_l} = G_k(X) \sigma \beta_{kl}, \quad \forall X \in R^n,$$

where $\sigma = \frac{\tau(\eta + \delta\gamma)}{\eta(\alpha + \gamma)}$. Alternatively, it can be rewritten as a compact matrix form

$$DG(X) = \text{diag}(G(X)) \sigma A, \quad X \in R^n, \quad (14)$$

where $Dh(x)$ represents the derivative of a function $h(x)$ with respect to x .

The monotony of G implies the monotony of DG ; that is, for each $0 \leq X \leq Y \leq \xi$ and a vector $B \geq 0$, it holds that

$$DG(X)B \leq DG(Y)B.$$

Combining this with $G(\xi^-) = \xi^-$ and $G(\xi^+) = \xi^+$, we have $DG(\xi^-) = \text{diag}(\xi^-) \sigma A$ and $DG(\xi^+) = \text{diag}(\xi^+) \sigma A$.

The result of a unique solution for (13) in $[0, \xi]$ is summarized as follows.

Theorem 2.6 *Assume that $\alpha + \gamma > 0$, $\eta > 0$ and $0 \leq \epsilon_k < 1$, $k = 1, \dots, n$. Assume in addition that A is a nonnegative irreducible matrix, i.e., a node of degree k can be connected by any other node of degree l ($l \neq k$). Then, it holds that*

- (a) $G(\xi) = \xi$ if and only if $\epsilon_k = 0$, $k = 1, \dots, n$;
- (b) If $\epsilon_k > 0$ for some $k = 1, \dots, n$, then it admits a unique fixed point ξ^* of G in the interval $(0, \xi)$.

Proof Since A is a nonnegative irreducible matrix and $\xi^+ \gg 0$, we conclude that $DG(\xi^+) = \text{diag}(\xi^+) \sigma A$ is also a nonnegative irreducible matrix.

Proof of (a): First, we show that G has a fixed point $\xi \gg 0$ if and only if $\epsilon_k = 0$, $k = 1, \dots, n$. To see this, $G(\xi) = \xi$ implies that

$$\begin{cases} (1 - \epsilon_1) \exp \left\{ -\sigma \sum_{l=1}^n \beta_{1l} \epsilon_l \right\} = 1 - \epsilon_1, \\ \vdots \\ (1 - \epsilon_n) \exp \left\{ -\sigma \sum_{l=1}^n \beta_{nl} \epsilon_l \right\} = 1 - \epsilon_n, \end{cases}$$

which is satisfied if and only if

$$\sigma \sum_{l=1}^n \beta_{kl} \epsilon_l = 0, \quad k = 1, \dots, n \Leftrightarrow A(1 - \xi) = 0.$$

Since matrix A is nonnegative irreducible and $0 \leq \epsilon_k < 1$, $k = 1, \dots, n$, we have $A(1 - \xi) = 0 \Leftrightarrow 1 - \xi = 0$, i.e., $\epsilon_k = 0$, $k = 1, \dots, n$.

Proof of (b): If $\epsilon_k > 0$ for some $k = 1, \dots, n$, it follows that $0 \ll G(\xi) < \xi$ and $\xi^+ < \xi$. Moreover, using the monotony of G yields $\xi^+ = G(\xi^+) \leq G(\xi)$.

To show that a unique fixed point ξ^* of G exists whenever $\epsilon_k > 0$ for some $k = 1, \dots, n$, we only need to verify that $\xi^- = \xi^+$. Suppose not, that is, $\xi^- < \xi^+$, then it follows that

$$\xi^+ - \xi^- = G(\xi^+) - G(\xi^-) = \int_0^1 DG(\xi^- + \lambda(\xi^+ - \xi^-))(\xi^+ - \xi^-) d\lambda.$$

Since DG is monotone increasing for all $\lambda \in [0, 1]$

$$DG(\xi^- + \lambda(\xi^+ - \xi^-))(\xi^+ - \xi^-) \leq DG(\xi^+)(\xi^+ - \xi^-)$$

so that

$$\xi^+ - \xi^- \leq DG(\xi^+)(\xi^+ - \xi^-). \quad (15)$$

Since $DG(\xi^+)$ is a nonnegative irreducible matrix (Berman and Plemmons 1994), there must exist a left eigenvector $V \gg 0$ such that $V^T DG(\xi^+) = \rho(DG(\xi^+))V^T$. Thus, we have

$$V^T(\xi^+ - \xi^-) \leq V^T DF(\xi^+)(\xi^+ - \xi^-) = \rho(DF(\xi^+))V^T(\xi^+ - \xi^-)$$

so that $\rho(DF(\xi^+)) \geq 1$, where the assumption $\xi^- < \xi^+$ is used.

On the other hand, taking into consideration the facts

$$G(\xi) - \xi^+ = G(\xi) - G(\xi^+) = \int_0^1 DG(\xi^+ + \lambda(\xi - \xi^+))(\xi - \xi^+) d\lambda,$$

and for all $\lambda \in [0, 1]$

$$DG(\xi^+ + \lambda(\xi - \xi^+))(\xi - \xi^+) \geq DG(\xi^+)(\xi - \xi^+),$$

we have

$$V^T(G(\xi) - \xi^+) \geq \rho(DF(\xi^+))V^T(\xi - \xi^+)$$

so that

$$V^T(G(\xi) - \xi^+) \geq V^T(\xi - \xi^+) \Rightarrow V^T G(\xi) \geq V^T \xi.$$

This contradicts with $0 \ll G(\xi) < \xi$. \square

Remark 2.7 Theorem 2.6 has two implications. Mathematically, it clarifies the existence and uniqueness of the solution for the final size Eq. (13). Biologically, it says that there will be no disease if and only if no initial infectious seeds exist. On the contrary, there will be a minor or major outbreak irrespective of the initial distribution of infectious seeds; that is, nodes of any degree can be infected independent of the initial distribution of infectious seeds.

Remark 2.8 Theorem 2.6 shows that the solution of (13) is unique, and since the map G is monotone increasing on the interval the unique solution can be obtained through an iteration. Thus, it provides a numerical algorithm to estimate the final epidemic size Z in annealed networks, i.e., $Z = \sum_k P(k)R_k(+\infty)$. Using $R_k(+\infty) = 1 - S_k(+\infty)$ gives $Z = 1 - \sum_k P(k)S_k(+\infty)$, where the final density of susceptible nodes in each degree class k is calculated numerically as

$$S_k(+\infty) = \lim_{j \rightarrow +\infty} G_k^j(1 - \epsilon_k).$$

In particular, if $\epsilon_k > 0$ for some $k = 1, \dots, n$, according to Theorem 2.6 (b), we may use the formula $S_k(+\infty) = \lim_{j \rightarrow +\infty} G_k^j(0)$ to compute the final density of susceptible nodes with degree k . Moreover, if matrix A is non-irreducible and nonnegative, i.e., the network is disconnected, we can use the above result to each isolated connected component whose connectivity matrix is irreducible and nonnegative.

2.3 Edge-Based Sitr Model in Annealed Networks

On the other hand, Eq. (6) can be rewritten as

$$\frac{S_k(t)}{S_k(0)} = \frac{S_k(t)}{1 - \epsilon_k} = e^{-\tau \sum_l \beta_{kl} \int_0^t (I_l(s) + \delta T_l(s)) ds},$$

which can be interpreted as the probability that an initial susceptible node of degree k is still susceptible at time t . To obtain more useful information for epidemic spreading with treatment, it is necessary to specify the conditional probability $P(l|k)$. One possibility is degree uncorrelated mixing, that is, $\beta_{kl} = klP(l)/\langle k \rangle$. Under the assumption of degree uncorrelated mixing, we may let $\theta(t) = e^{-\tau \sum_l \int_0^t (lP(l)I_l(s)/\langle k \rangle + \delta lP(l)T_l(s)/\langle k \rangle) ds}$,

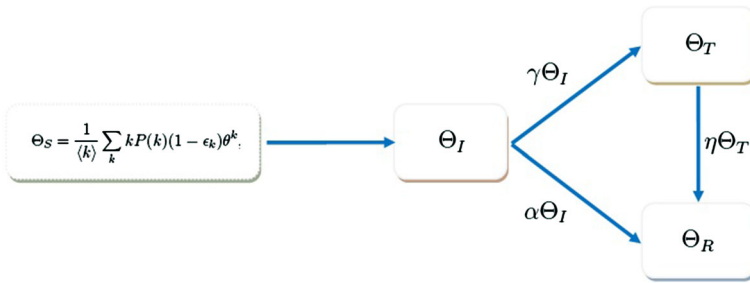


Fig. 2 Flow diagram for the heterogeneous mixing SITR model in degree uncorrelated annealed networks. The variables Θ_S , Θ_I , Θ_T and Θ_R are the fraction of stubs that emanate from susceptible, infected, treated and recovered nodes, respectively (Online version in color)

which can be regarded as the probability that a stub or half edge has never spread infection to the node under consideration, customarily called the test node, from any direct neighbor. Thus, it follows that $S_k(t) = (1 - \epsilon_k)\theta^k(t)$ and $S(t) = \sum_k (1 - \epsilon_k)P(k)\theta^k(t)$.

To close the equation of $S_k(t)$ or $S(t)$, we need the equation satisfied by $\theta(t)$. Denote by ϕ_S , ϕ_I , ϕ_T and ϕ_R the probability that a stub has never spread infection to the test node and additionally the current neighbor is susceptible, infected, treated and recovered, respectively. In annealed networks, since a (test) node connects to a new neighbor at each moment, the probability that it connects to a node of a given status equals the fraction of all stubs emanating from nodes of that status. Hence, we must consider the fraction of stubs that emanate from susceptible, infected, treated and recovered nodes Θ_S , Θ_I , Θ_T and Θ_R , respectively. Since the neighbors change rapidly, the following relations hold: $\phi_S = \theta\Theta_S$, $\phi_I = \theta\Theta_I$, $\phi_T = \theta\Theta_T$ and $\phi_R = \theta\Theta_R$. For example, ϕ_S is the product of the probability θ that a stub has never traversed infection with the probability Θ_S that it currently connects to a susceptible node.

The flow diagram between Θ_S , Θ_I , Θ_T and Θ_R is depicted in Fig. 2. The transitions between compartments S , I , T and R are similar to Fig. 1, and the variable S can be computed in terms of ϵ_k and θ . Using the assumption that the neighbors connected to a single stub any two times are independent (since partnerships are fleeting), we find none fluxes among ϕ_S , ϕ_I , ϕ_T and ϕ_R . The partnerships terminating and forming rapidly, rather than infection or recovery of the partner, result in the change for partner status. We need transitions for variables Θ_S , Θ_I , Θ_T and Θ_R . We compute Θ_S directly as follows. The probability that a stub emanates from a node of degree k is $kP(k)/\langle k \rangle$, the probability the node is susceptible at the initial time is $1 - \epsilon_k$, and the probability the node is susceptible by time t is $\theta^k(t)$. Thus, it follows that $\Theta_S = \langle k \rangle^{-1} \sum_k kP(k)(1 - \epsilon_k)\theta^k$, a weighted summation. Stubs belonging to susceptible nodes change into stubs belonging to infected nodes if the susceptible nodes are no longer susceptible. Stubs emanating from infected nodes become stubs emanating from treated nodes at rate γ and stubs emanating from treated nodes become stubs emanating from recovered nodes at rate η , thus $\Theta'_T = \gamma\Theta_I - \eta\Theta_T$. Finally, $\Theta_I = 1 - \Theta_S - \Theta_T - \Theta_R$.

The probability θ decreases due to the infection spread across a stub, either from the infected or treated nodes. Then,

$$\theta' = -\tau\phi_I - \delta\tau\phi_T. \quad (16)$$

Substituting $\phi_I = \theta\Theta_I$ and $\phi_T = \theta\Theta_T$ into Eq. (16) yields

$$\theta' = -\tau\theta\Theta_I - \delta\tau\theta\Theta_T. \quad (17)$$

Next, we are ready to find equations for Θ_I and Θ_T . Noting that $\Theta'_I = -\Theta'_S - (\alpha + \gamma)\Theta_I$, we first compute Θ_I directly. Using the expression for Θ_S , we have

$$\Theta'_I = \tau\theta(\Theta_I + \delta\Theta_T) \frac{1}{\langle k \rangle} \sum_k k^2 P(k)(1 - \epsilon_k)\theta^{k-1} - (\alpha + \gamma)\Theta_I. \quad (18)$$

Therefore, the full system governing Sitr dynamics in annealed networks with arbitrary degree distribution and no degree correlation is given by

$$\begin{cases} \theta' = -\tau\theta(\Theta_I + \delta\Theta_T), \\ \Theta'_I = \tau\theta(\Theta_I + \delta\Theta_T) \frac{1}{\langle k \rangle} \sum_k k^2 P(k)(1 - \epsilon_k)\theta^{k-1} - (\alpha + \gamma)\Theta_I, \\ \Theta'_T = \gamma\Theta_I - \eta\Theta_T, \\ S = \sum_k (1 - \epsilon_k)P(k)\theta^k, \\ I' = \tau\theta(\Theta_I + \delta\Theta_T) \sum_k kP(k)(1 - \epsilon_k)\theta^{k-1} - (\alpha + \gamma)I, \\ T' = \gamma I - \eta T. \end{cases} \quad (19)$$

The initial conditions are $\theta(0) = 1$, $\Theta_I(0) = \sum_k kP(k)\epsilon_k/\langle k \rangle$, $\Theta_T(0) = 0$, $I(0) = \sum_k P(k)\epsilon_k$ and $T(0) = 0$.

To obtain the basic reproduction number R_0 for model (19), we employ the next generation matrix method introduced in previous subsection. Specifically, only variables Θ_I and Θ_T are involved. Linearizing the second and third equations of (19) about the disease-free equilibrium ($\theta = 1$, $\Theta_I = 0$ and $\Theta_T = 0$), we have

$$\begin{cases} \Theta'_I = \tau \frac{1}{\langle k \rangle} \sum_k k^2 P(k)(1 - \epsilon_k)(\Theta_I + \delta\Theta_T) - (\alpha + \gamma)\Theta_I, \\ \Theta'_T = \gamma\Theta_I - \eta\Theta_T. \end{cases} \quad (20)$$

Letting $\epsilon_k \rightarrow 0$ (corresponding to infinitesimal initial infection), $k = 1, 2, \dots$, and rewriting (20) in a matrix form, we have

$$\frac{d}{dt} \begin{pmatrix} \Theta_I \\ \Theta_T \end{pmatrix} = (F_1 - V_1) \begin{pmatrix} \Theta_I \\ \Theta_T \end{pmatrix},$$

where

$$F_1 = \begin{bmatrix} \tau \frac{\langle k^2 \rangle}{\langle k \rangle} & \delta\tau \frac{\langle k^2 \rangle}{\langle k \rangle} \\ 0 & 0 \end{bmatrix} \text{ and } V_1 = \begin{bmatrix} \alpha + \gamma & 0 \\ -\gamma & \eta \end{bmatrix}.$$

Then, it follows that

$$F_1 V_1^{-1} = \begin{bmatrix} \left(\frac{\tau}{\alpha + \gamma} + \frac{\gamma}{\alpha + \gamma} \frac{\delta \tau}{\eta} \right) \frac{\langle k^2 \rangle}{\langle k \rangle} & \frac{\delta \tau}{\eta} \frac{\langle k^2 \rangle}{\langle k \rangle} \\ 0 & 0 \end{bmatrix}.$$

Hence,

$$R_0 = \rho(F_1 V_1^{-1}) = \left(\frac{\tau}{\alpha + \gamma} + \frac{\gamma}{\alpha + \gamma} \frac{\delta \tau}{\eta} \right) \frac{\langle k^2 \rangle}{\langle k \rangle},$$

which is the exact expression as that obtained (4) for degree uncorrelated case.

To obtain the final size equation for model (19), we need to find $\theta(+\infty)$. The expression of $\theta(t)$ can be rewritten as

$$\ln \theta(t) = -\tau \int_0^t (\Theta_I(s) + \delta \Theta_T(s)) ds.$$

Noting that $\Theta'_S + \Theta'_I = -(\alpha + \gamma)\Theta_I$, we integrate it from 0 to t and have

$$\Theta_S(t) + \Theta_I(t) - 1 = -(\alpha + \gamma) \int_0^t \Theta_I(s) ds, \quad t > 0. \quad (21)$$

Similarly, from the observation $\Theta'_S + \Theta'_I + \Theta'_T = -\alpha\Theta_I - \eta\Theta_T$, we have

$$\Theta_S(t) + \Theta_I(t) + \Theta_T(t) - 1 = -\alpha \int_0^t \Theta_I(s) ds - \eta \int_0^t \Theta_T(s) ds, \quad t > 0. \quad (22)$$

Hence, Eq. (21) gives

$$\int_0^t \Theta_I(s) ds = \frac{1}{\alpha + \gamma} - \frac{1}{\alpha + \gamma} (\Theta_S(t) + \Theta_I(t)). \quad (23)$$

Inserting Eq. (23) into Eq. (22) yields

$$\int_0^t \Theta_T(s) ds = \frac{1}{\eta} - \frac{1}{\eta} (\Theta_S(t) + \Theta_I(t) + \Theta_T(t)) - \frac{\alpha}{\eta(\alpha + \gamma)} (1 - \Theta_S(t) - \Theta_I(t)). \quad (24)$$

Substituting Eqs. (23) and (24) into the expression of $\ln \theta(t)$ gives

$$\ln \theta(t) = \frac{\tau(\eta + \delta\gamma)}{\eta(\alpha + \gamma)} (\Theta_S(t) + \Theta_I(t) - 1) + \frac{\delta\tau}{\eta} \Theta_T(t). \quad (25)$$

Letting $t \rightarrow +\infty$ and using $\Theta_I(+\infty) = \Theta_T(+\infty) = 0$, we have

$$\theta(+\infty) = e^{-\sigma(1-\Theta_S(+\infty))} = e^{-\sigma\{1-\langle k \rangle^{-1} \sum_k k P(k)(1-\epsilon_k)\theta^k(+\infty)\}}. \quad (26)$$

Thus, the final size equation is given by

$$R(+\infty) = 1 - S(+\infty) = 1 - \sum_k (1 - \epsilon_k) P(k) \theta^k(+\infty), \quad (27)$$

where $\theta(+\infty)$ can be solved from Eq. (26).

Let $H(x) = e^{-\sigma\{1-\langle k \rangle^{-1} \sum_k k P(k)(1-\epsilon_k)x^k\}}$, $x \in (0, 1]$. The next step is to show that the fixed point equation $x = H(x)$ has a unique solution $x^* \in (0, 1)$ for any $\epsilon_k \in (0, 1]$, $k = 1, \dots, n$. In the case when there are no infected individuals at the initial time, i.e., $\sum_k \epsilon_k = 0$, all individuals are susceptible, then we have the trivial solution $x_0 = 1$ and $R(+\infty) = 0$. The more interesting case is to consider the limit $R(+\infty)$ as $\sum_k \epsilon_k$ tends to zero. If the limit $R(+\infty)$ is zero then there is no epidemic with an infinitesimal initial infection. However, if the limit is positive, implying that even an infinitesimal initial infection can give a positive final epidemic size. We have the following main result.

Theorem 2.9 Assume that $\alpha + \gamma > 0$ and $\eta > 0$. Then, it holds that

- (a) $H(1) = 1$ (i.e. with 1 as a fixed point) if and only if $\epsilon_k = 0$, $k = 1, \dots, n$;
- (b) If $\sum_k \epsilon_k = 0$ and $R_0 > 1$, then there exists another unique fixed point of H in $(0, 1)$, whereas $R_0 \leq 1$ there exists the trivial fixed point only and $H(x) > x$ in $(0, 1)$;
- (c) If $\epsilon_k > 0$ for some $k = 1, \dots, n$, i.e. $\sum_k \epsilon_k > 0$, then it admits a unique fixed point x^* of H in $(0, 1)$, moreover, $H(x) > x$ in $(0, x^*)$ and $H(x) < x$ in $(x^*, 1)$.

Proof By direct calculation, we have

$$H'(x) = (\sigma \langle k \rangle^{-1} \sum_k k^2 P(k)(1 - \epsilon_k)x^{k-1}) e^{-\sigma\{1-\langle k \rangle^{-1} \sum_k k P(k)(1-\epsilon_k)x^k\}} \geq 0,$$

implying that H is monotone increasing. In particular, if $\epsilon_k < 1$ for some $k = 1, \dots, n$, then H is strictly increasing.

Proof of (a): We verify that $x_0 = 1$ is a fixed point of H if and only if $\epsilon_k = 0$, $k = 1, \dots, n$. In fact, $H(1) = 1$ implies that $e^{-\sigma\{1-\langle k \rangle^{-1} \sum_k k P(k)(1-\epsilon_k)\}} = 1$, which is satisfied if and only if

$$\sigma\{1 - \langle k \rangle^{-1} \sum_k k P(k)(1 - \epsilon_k)\} = 0 \Leftrightarrow \epsilon_k = 0, \quad k = 1, \dots, n.$$

Proof of (b): We have $0 < H(0) = e^{-\sigma} < 1$ and $H(1) = e^{-\sigma \langle k \rangle^{-1} \sum_k k P(k) \epsilon_k} \leq 1$. If $\sum_k \epsilon_k = 0$, then by (a) we have $H(1) = 1$ and H is strictly increasing, i.e. $H'(x) > 0$. To show the existence and uniqueness of another fixed point of H in $(0, 1)$, we need the second derivative of H . Direct calculation gives $H''(x) = (h'(x) + h''(x))e^{h(x)}$, where $h(x) = -\sigma + \sigma \langle k \rangle^{-1} \sum_k k P(k)(1 - \epsilon_k)x^k$ is a polynomial with positive coefficients except the constant term. Hence, $h'(x) > 0$, $h''(x) > 0$ and $H''(x) > 0$, meaning that H strictly convex in $(0, 1)$, that is, $H'(x)$ is strictly increasing in $(0, 1)$.

Since $H'(0) = 0$ and $H'(x)$ is continuous in $[0, 1]$, the existence of a fixed point of H in $(0, 1)$ is determined by $H'(1)$. In fact, if $H'(1) > 1$, by the convexity of H and continuity of H' there exists a unique $x_1^* \in (0, 1)$ such that $H'(x_1^*) = 1$, moreover $H'(x) < 1$ for $x \in (0, x_1^*)$ and $H'(x) > 1$ for $x \in (x_1^*, 1)$. Let $g(x) = H(x) - x$. Since $g'(x) = H'(x) - 1 > 0$ in $(x_1^*, 1)$, $g(x)$ is strictly increasing in the open interval $(x_1^*, 1)$. It follows that $g(x) < g(1) = 0$ in $(x_1^*, 1)$, i.e. $H(x) < x$ in $(x_1^*, 1)$, meaning that the graph of $H(x)$ is below that of x if x is close to 1. However, $0 < H(0) < 1$, meaning that the graph of $H(x)$ is above that of x if x is close to 0. Therefore, by the continuity and monotonicity of H there must exist a unique fixed point in $(0, 1)$.

On the other hand, if $H'(1) \leq 1$, then $H'(x) < H'(1) \leq 1$ and $g'(x) < 0$ for $x \in (0, 1)$. That is, $g(x)$ is strictly decreasing in $(0, 1)$. Hence, $g(x) > g(1) = 0$, i.e. $H(x) > x$ in $(0, 1)$. Moreover, substituting $\epsilon_k = 0$, $k = 1, \dots, n$ and $x = 1$ into $H'(x)$, we have $H'(1) = \sigma \langle k^2 \rangle / \langle k \rangle$, which is exactly the basic reproduction number R_0 .

Proof of (c): Note that $0 < H(0) < 1$. If $\epsilon_k > 0$ for some $k = 1, \dots, n$, then $0 < H(1) = e^{-\sigma \langle k \rangle^{-1} \sum_k k P(k) \epsilon_k} < 1$. This implies that the graph of $H(x)$ begins above that of x and ends below that of x in the interval $[0, 1]$. Hence, by the continuity and monotonicity of H there must exist a unique fixed point x^* in the open interval $(0, 1)$. \square

Remark 2.10 Using the method in Wang et al. (2018), model (19) can be easily extended to SITR dynamics in degree correlated annealed networks. In this case, the probability that a stub of degree k node has not yet traversed infection should be associated with its degree, i.e., θ_k . Then, the final size equations are composed of a system of n nonlinear equations.

Remark 2.11 For degree uncorrelated mixing in annealed networks, i.e., $P(l|k) = lP(l)/\langle k \rangle$, the final size Eq. (13) contains n nonlinear equations, and Theorem 2.6 requires that the connectivity matrix A be irreducible. However, Theorem 2.9 does not have this requirement. Hence, in this sense, results of Theorem 2.9 are more general.

Remark 2.12 Theorem 2.9 provides a numerical algorithm to estimate the final epidemic size Z in degree uncorrelated annealed networks. In particular, if $\epsilon_k > 0$ for some $k = 1, \dots, n$ or $\sum_k \epsilon_k = 0$ and $R_0 > 1$, there exists a unique fixed point $x^* \in (0, 1)$ of the function $H(x)$, and the sequence defined by the iteration $x_{j+1} = H(x_j)$ for any initial value $x_0 \in (0, 1)$ converges to x^* . In fact, if $x_0 = x^*$, then $x_j = x^*$ for all j , and the result follows. If $x_0 < x^*$, then by the strict monotonicity of H , $x_j < x^*$ implies $x_{j+1} = H(x_j) < H(x^*) = x^*$. On the other hand, $x_j < x^*$ gives $x_{j+1} = H(x_j) > x_j$ for all j , meaning that the sequence is increasing, thus it converges to x^* . Similarly, if $x_0 > x^*$, it can be proven that $x_j > x^*$ for all j and the sequence is decreasing.

In the following, we will implement some numerical simulations for the model (19) in order to show more network epidemiological insights. Based on the insightful work about 1957 influenza pandemic in Brauer (2008), the disease parameters in model (19) are taken as: $\delta = 0.2$, $\alpha = 0.244$, $\gamma = 0.8$ and $\eta = 0.323$. We present the results obtained by simulating the differential Eq. (19).

In Brauer (2008), a homogeneous mixing population of size $N = 2000$ (including 12 infectives initially) is used for simulations. We use a heterogeneous mixing population of size $N = 6000$ with different initial fraction of infectives. For the sake of convenience, we let $\epsilon_k = \epsilon$, $k = 1, \dots, n$, that is, a fraction ϵ of total nodes is set to be infected at the initial time independent of their degrees.

We generate a degree sequence with Poisson degree distribution, and the mean degree of the annealed network obtained is $\langle k \rangle = 5.989$. Let $\tau = 0.09$, then $R_0 = 0.901 < 1$. In Fig. 3, we show some phase plane representations of the relation between the fraction of susceptible S nodes and the fraction of infected I or treated T nodes, respectively, which also illustrate Theorem 2.9 about the final epidemic size (intersection of the horizontal axis). In these figures the disease and network parameters are fixed while the initial fraction of infected nodes are varying with $\epsilon = 0.1, 0.2$ and 0.3 , respectively. From the figures, it can be seen that the limit $S(+\infty)$ is an decreasing function of ϵ if $R_0 < 1$, which cannot be seen easily from the expression of $S(t)$ in (19). Note that the fraction of treated nodes may not be a decreasing function of time t even if $R_0 < 1$. To see this, we plot the fraction of infected and the fraction of treated nodes for system (19) with varying ϵ in Fig. 4. Specifically, the function $T(t)$ first increases to reach a peak, then decreases to 0 finally. This shows that the dynamical behavior of the treated class is more complex than that of the infected class even if $R_0 < 1$. Our low dimensional SITR model in annealed networks provides a fast numerical estimation of the peak and arrival time of peak size for individuals to be treated, which can guide the public health department to allocate medical resource reasonably and thus accelerate the extinction of a disease.

In Figs. 5 and 6, we plot some phase plane representations of the solutions of system (19) and time evolution of the fraction of infected and treated nodes in a Poisson network, respectively. In all these figures, the disease parameters are the same as in Fig. 3 except $\tau = 0.12$, resulting in $R_0 = 1.201 > 1$, and the network parameters are not changed while the initial fraction of infected nodes are varying with $\epsilon = 0.001, 0.01$, and 0.1 , respectively. Obviously, as the infection rate τ increases, the peak size of the treated class increases. However, one may observe that even if $R_0 > 1$ the function $I(t)$ may first decrease, then increase to reach a peak and decrease to 0 finally (see, for example, the dotted line in Fig. 6 corresponding to $\epsilon = 0.01$). As ϵ increases, the qualitative behavior of infected class changes, for example, when $\epsilon = 0.1$ the function $I(t)$ is always decreasing and tends to 0 finally. In fact, we obtain the basic reproduction number R_0 as $\epsilon \rightarrow 0$, and when $\epsilon = 0.1$ (the initial infection is not infinitesimal and cannot be ignored) the effective reproduction number is $(1 - \epsilon) * R_0$.

Figure 6 shows that the dynamical behavior of infected class is affected by the initial infection conditions. If we further increase the infection rate τ , the dynamics of infected class becomes simpler.

In Fig. 7, we plot some phase plane representations of the relation between the fraction of susceptible nodes and the fraction of infected or treated nodes, respectively. The network and disease parameters are the same as above except $\tau = 0.3$, resulting in $R_0 = 3.004 > 1$. It can be seen that the qualitative behavior of the function $I(t)$ has little change when $\epsilon = 0.001$ and 0.01 . Comparing with Fig. 5, the qualitative behavior of the function $I(t)$ is also dependent on the infection rate τ . Figure 8 clearly shows that the function $I(t)$ first increases to reach a peak and then decreases to 0

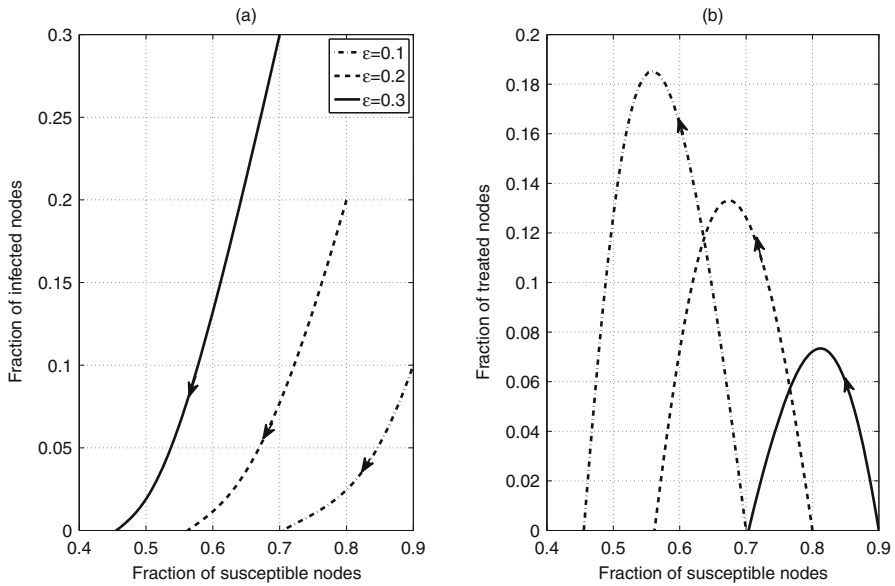


Fig. 3 Phase plane representations of the relation between the fraction of susceptible nodes and the fraction of infected (a) or treated (b) nodes in a network with Poisson degree distribution, respectively. Model parameters are: $\tau = 0.09$, $\delta = 0.2$, $\alpha = 0.244$, $\gamma = 0.8$ and $\eta = 0.323$. The fraction of initial infected nodes takes varying values $\epsilon = 0.1, 0.2$ and 0.3 , respectively, while the fraction of susceptible nodes satisfies $S(0) = 1 - \epsilon$ (Online version in color)

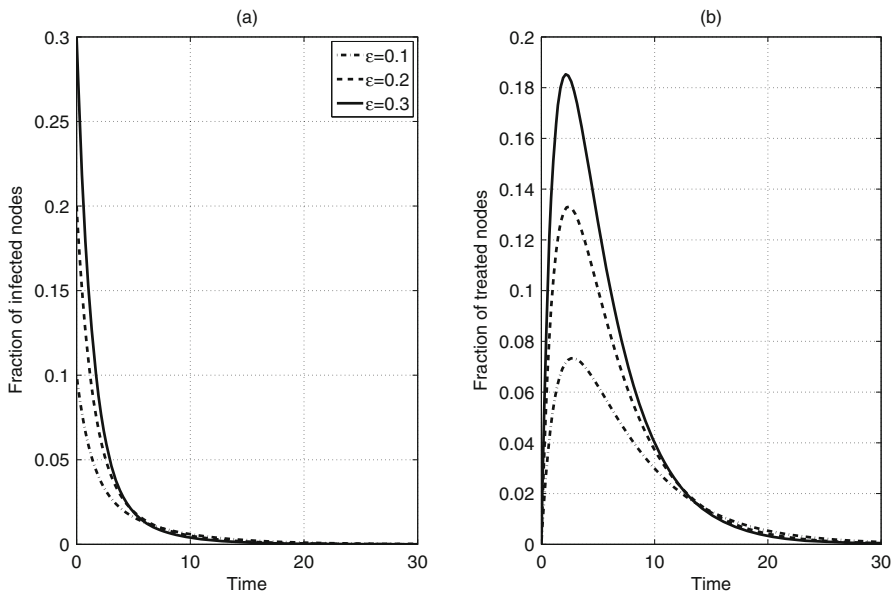


Fig. 4 Time evolution of the fraction of infected (a) and treated (b) nodes in a network with Poisson degree distribution, respectively. The disease and network parameters are the same as those in Fig. 3. The function $T(t)$ is increasing to reach a peak, then decreasing to 0 finally even if $R_0 < 1$ (Online version in color)

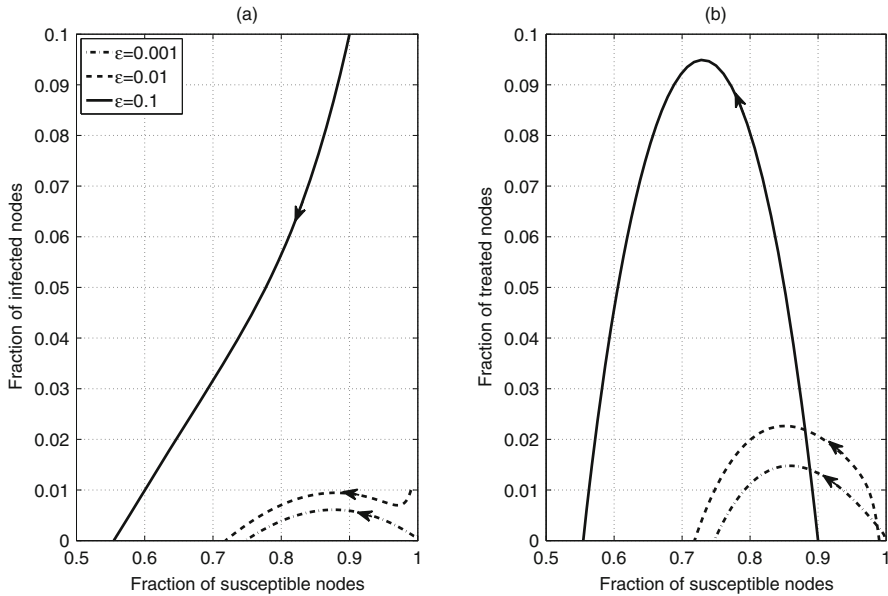


Fig. 5 Phase plane representations of the relation between the fraction of susceptible nodes and the fraction of infected (a) or treated (b) nodes in the same network as in Fig. 3. The disease parameters are the same as in Fig. 3 except $\tau = 0.12$. The fraction of infected nodes takes varying values $\epsilon = 0.001, 0.01$ and 0.1 , respectively, while the fraction of susceptible nodes satisfies $S(0) = 1 - \epsilon$ (Online version in color)

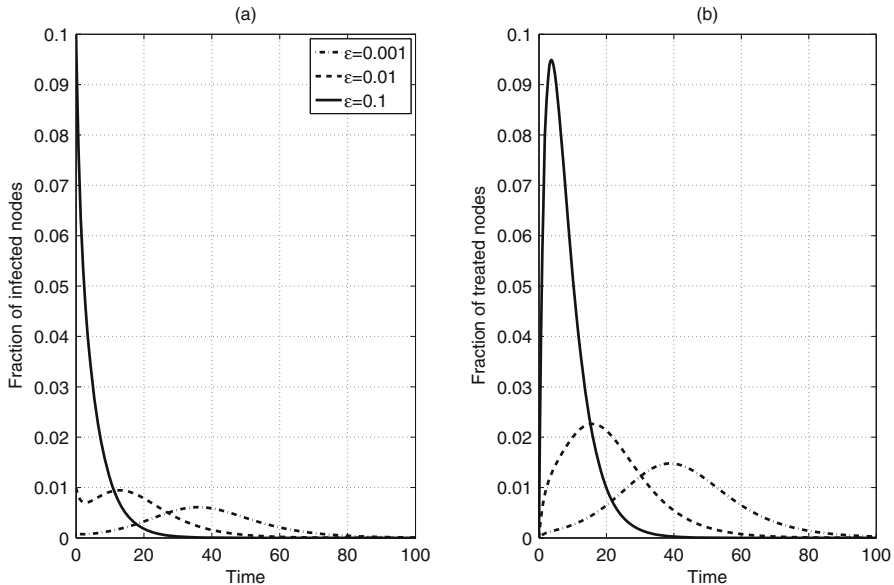


Fig. 6 Time evolution of the fraction of infected (a) and treated (b) nodes in a network with Poisson degree distribution, respectively. The disease and network parameters are the same as those in Fig. 5. The function $I(t)$ may be decreasing, then increasing to reach a peak, and finally decreasing to 0. The dynamical behavior of the function $I(t)$ is dependent on the initial conditions (Online version in color)

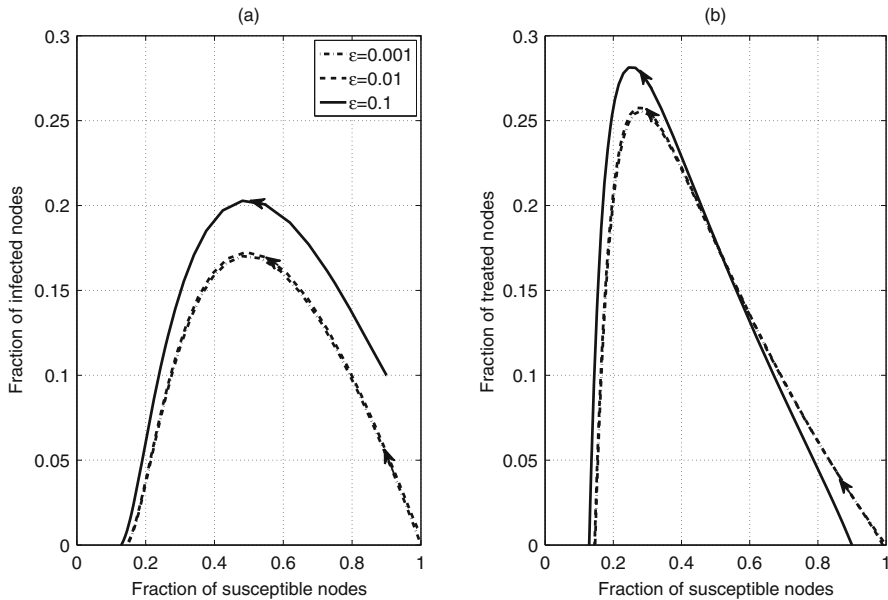


Fig. 7 Phase plane representations of the relation between the fraction of susceptible nodes and the fraction of infected (a) or treated (b) nodes in the same network as in Fig. 3. The disease parameters are the same as in Fig. 3 except $\tau = 0.3$. The fraction of infected nodes takes varying values $\epsilon = 0.001, 0.01$ and 0.1 , respectively, while the fraction of susceptible nodes satisfies $S(0) = 1 - \epsilon$ (Online version in color)

finally, that is, there is a single outbreak. This kind of behavior is similar to that of the function $I(t)$ for the classical SIR model when $R_0 > 1$.

We now generate a degree sequence with scale-free degree distribution and observe how this degree distribution affects the phase plane solutions of system (19) and the disease dynamics. The network parameters are taken as: $N = 6000$, minimum degree $k_{\min} = 2$, maximum degree $k_{\max} = 75$ and degree exponent $\nu = 2.02$ ($P(k) \propto k^{-\nu}$). The mean degree of a generated network is $\langle k \rangle = 5.996$, and the second moment is $\langle k^2 \rangle = 106.94$. Let $\tau = 0.12$, and the other disease parameters be the same as above, then $R_0 = 3.066 > 1$. In Fig. 9, we show some phase plane representations of the relation between the fraction of susceptible S nodes and the fraction of infected I or treated T nodes, respectively, which also illustrate Theorem 2.9 on the information of the final epidemic size (intersection of the horizontal axis). Moreover, comparing with Fig. 5, we notice that the heterogeneity of contact number may alter the qualitative behavior of phase plane solutions (see, for example, the solid line corresponding to $\epsilon = 0.1$). In Fig. 10, we present the fraction of infected and the fraction of treated nodes for system (19) with varying ϵ , respectively. Obviously, a higher heterogeneity in degree distribution tends to increase the basic reproduction number and the peak size (if it exists) while decreasing the arrival time of the peak.

Finally, we can find that as degree heterogeneity increases, the influence of degree distribution on the disease dynamics is getting sensitive. More precisely, in Figs. 6 and 10, the disease parameters are the same, and the mean degree of the two annealed

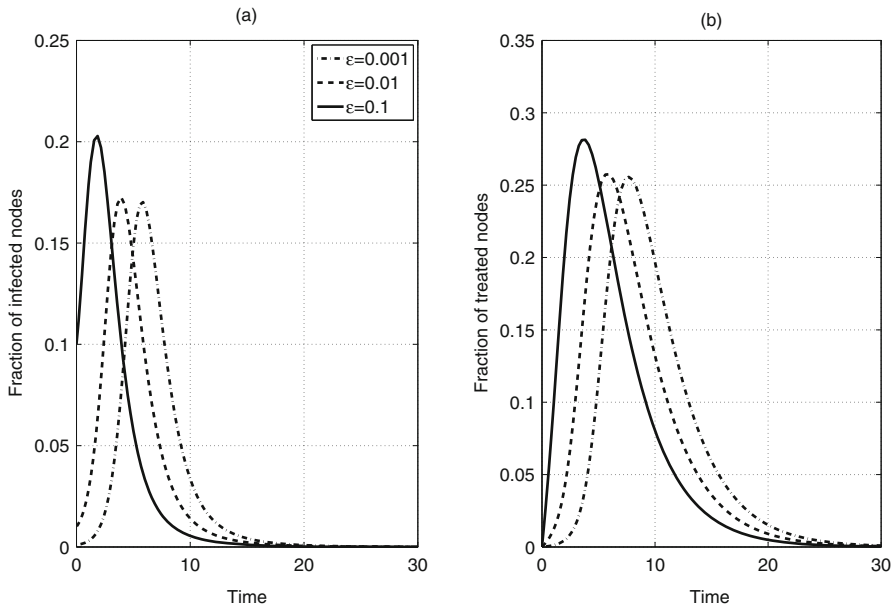


Fig. 8 Time evolution of the fraction of infected (a) and treated (b) nodes in a network with Poisson degree distribution, respectively. The disease and network parameters are the same as those in Fig. 7. This kind of behavior is similar to that of $I(t)$ for the classical SIR model when $R_0 > 1$ (Online version in color)

networks are almost the same, however, the qualitative behavior of the infected class $I(t)$ is quite different. For example, in the case of $\epsilon = 0.1$, the function $I(t)$ decreases to 0 directly in Fig. 6 while the function $I(t)$ may change the convexity in Fig. 10.

3 Epidemic Models with Treatment in Quenched Networks

Quenched network models mean that the network dynamics evolves much slower than the dynamical processes in them. In other words, the nodes and edges of a network are static or fixed. In particular, the neighbors of a node are fixed and the status correlations between individuals may appear during the spread of a disease. Usually, the correlations among individuals of different states can be well captured by the edge-based compartmental (EBC) approach (Volz 2008; Miller et al. 2012) or the quenched mean-field (QMF) theory (Mieghem et al. 2009).

3.1 Edge-Based Sitr Model in Quenched Networks

We now consider Sitr dynamics in quenched networks of configuration type, i.e. no clustering or degree correlations. Here, we use an edge-based modeling approach in Miller et al. (2012) to obtain a nonlinear system of low-dimensional ordinary differential equations.

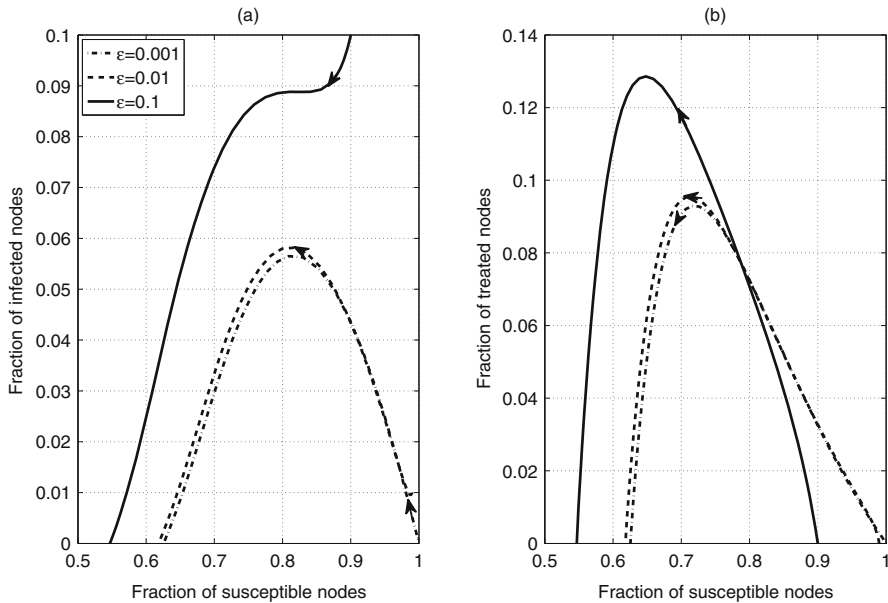


Fig. 9 Phase plane representations of the relation between the fraction of susceptible nodes and the fraction of infected (a) or treated (b) nodes in a network with scale-free degree distribution, respectively. The disease parameters are the same as in Fig. 3 except $\tau = 0.12$. The fraction of initial infected nodes takes varying values $\epsilon = 0.001, 0.01$ and 0.1 , respectively, while the fraction of susceptible nodes satisfies $S(0) = 1 - \epsilon$ (Online version in color)

A susceptible node can be infected only through its direct neighbors, among whom there are infected or treated nodes. Specifically, by means of mean-field theory, susceptible nodes of degree k are governed statistically by

$$S'_k = -\tau k S_k p_I - \delta \tau k S_k p_T, \quad (28)$$

where $p_I = M_{SI}/M_S$ and $p_T = M_{ST}/M_S$ are the probability that an arc (each undirected edge corresponding to two directed arcs) with a susceptible ego connects to an infected alter and treated alter, respectively. For the ordered arc (u, v) in a network, the first node is usually called the *ego* and the second is the *alter*.

Dividing both sides of Eq. (28) by S_k and integrating it from 0 to t yield

$$\frac{S_k(t)}{S_k(0)} = e^{-\tau k \int_0^t (p_I(s) + \delta p_T(s)) ds} = \theta^k(t), \quad (29)$$

where $\theta(t) \doteq e^{-\tau \int_0^t (p_I(s) + \delta p_T(s)) ds}$ is the probability that a randomly chosen edge has not traversed the infection by time t . Then, it follows that $S_k(t) = (1 - \epsilon_k) \theta^k(t)$ and $S(t) = \sum_k (1 - \epsilon_k) P(k) \theta^k(t)$.

To give the rate of change of θ , we require the rate of change of infection traversed along an edge, which will occur only if there is at least one infectious neighbors (infected or treated). Let ϕ_S, ϕ_I, ϕ_T and ϕ_R be the probability that the alter node of

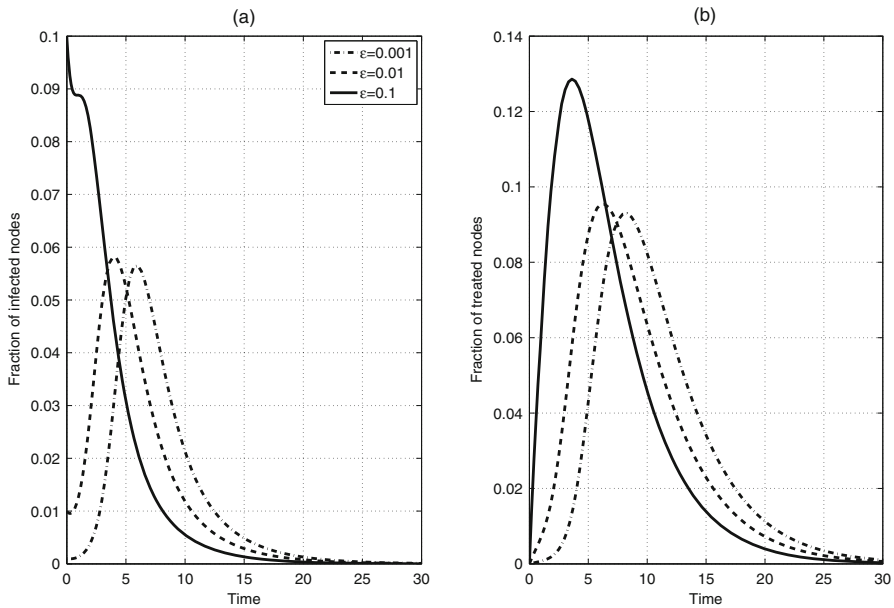


Fig. 10 Time evolution of the fraction of infected (a) and treated (b) nodes in a network with scale-free degree distribution, respectively. The disease and network parameters are the same as those in Fig. 9 (Online version in color)

an edge is susceptible, infected, treated and recovered, and the edge has not traversed the infection, respectively, for instance, $\phi_I = \theta p_I$. Obviously, edges that satisfy the definition of ϕ_x , $x \in \{S, I, T, R\}$, are a subset of edges that satisfy the definition of θ , i.e., $\theta(t) = \phi_S(t) + \phi_I(t) + \phi_T(t) + \phi_R(t)$.

The rate of change for θ decreases due to the infection crossing edges. Then,

$$\theta' = -\tau\phi_I - \delta\tau\phi_T. \quad (30)$$

To close the above system, we need equations for ϕ_I and ϕ_T . The probability ϕ_I decreases when infection traverses the edge or when the alter node is treated or recovers. On the other hand, the probability ϕ_I increases when the alter node becomes infectious, which equals the probability the alter node no longer being susceptible. Let $\kappa(t)$ be the probability a alter node is susceptible, then,

$$\phi_I' = -\tau\phi_I - (\alpha + \gamma)\phi_I - \kappa'(t).$$

We are ready to calculate $\kappa(t)$ directly. Noting the fact that in configuration type networks the probability a randomly chosen edge connects to a node of degree k is proportional to $kP(k)/\langle k \rangle$, and that the ego can only be infected by an edge other than

the one under consideration, we have

$$\kappa(t) = \sum_k \frac{kP(k)}{\langle k \rangle} (1 - \epsilon_k) \theta^{k-1}(t) = \frac{\sum_k kP(k)(1 - \epsilon_k) \theta^{k-1}}{\langle k \rangle}.$$

Thus, the equation for ϕ'_I becomes

$$\phi'_I = \tau(\phi_I + \delta\phi_T) \frac{1}{\langle k \rangle} \sum_k k(k-1)P(k)(1 - \epsilon_k) \theta^{k-2} - (\tau + \alpha + \gamma)\phi_I. \quad (31)$$

Similarly, the probability ϕ_T decreases when infection traverses the edge or when the alter node recovers. On the other hand, the probability ϕ_T increases when the alter node of infected status is treated.

$$\phi'_T = \gamma\phi_I - (\delta\tau + \eta)\phi_T. \quad (32)$$

Consequently, the full system for Sitr dynamics in quenched networks with arbitrary degree distribution is given by

$$\begin{cases} \theta' = -\tau(\phi_I + \delta\phi_T), \\ \phi'_I = \tau(\phi_I + \delta\phi_T) \frac{1}{\langle k \rangle} \sum_k k(k-1)P(k)(1 - \epsilon_k) \theta^{k-2} - (\tau + \alpha + \gamma)\phi_I, \\ \phi'_T = \gamma\phi_I - (\delta\tau + \eta)\phi_T, \\ S = \sum_k (1 - \epsilon_k)P(k) \theta^k, \\ I' = \tau(\phi_I + \delta\phi_T) \sum_k kP(k)(1 - \epsilon_k) \theta^{k-1} - (\alpha + \gamma)I, \\ T' = \gamma I - \eta T. \end{cases} \quad (33)$$

The initial conditions are $\theta(0) = 1$, $\phi_I(0) = \sum_k kP(k)\epsilon_k/\langle k \rangle$, $\phi_T(0) = 0$, $I(0) = \sum_k P(k)\epsilon_k$ and $T(0) = 0$. Moreover, the fluxes among ϕ_S , ϕ_I , ϕ_T and ϕ_R are depicted in Fig. 11.

3.2 Comparison with Stochastic Simulations

In this subsection, we compare predictions of model (33) with ensemble means of stochastic simulations. Therefore, we use two simple networks of configuration type (Molloy and Reed 1995) to give insights. One is a random network with a Poisson degree distribution, and the other with a (truncated) power-law degree distribution (Barabási and Albert 1999). We employ the Gillespie method (Gillespie 1976) to simulate the epidemic process on contact networks.

Configuration type network For a network with N nodes, each node is attached with k “stubs” randomly drawn from a known degree distribution $P(k)$. Two stubs that are not from the same node or nodes that are already neighbors are randomly selected to be paired. This pairing process is repeated until no such stubs can be paired, and the leftover stubs are abandoned.

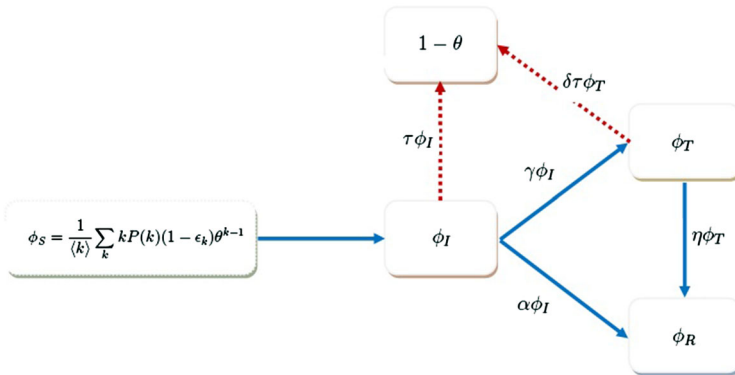


Fig. 11 Flow diagram for the heterogeneous mixing SITR model in quenched networks of configuration type. The variables ϕ_S , ϕ_I , ϕ_T and ϕ_R are the probability that the alter node of an edge is susceptible, infected, treated or recovered and has not transmitted the infection, respectively. The variable $1 - \theta$ is the probability that it has spread. The red dotted lines represent the fluxes between compartments ϕ and $1 - \theta$ resulting from infection of a neighbor of the ego. (Online version in color)

Simulating the epidemic process Each node is associated with its infection status, i.e., susceptible, infected, treated, or recovered. Initially, each node is labeled S , then a small fraction of nodes, say 0.1% of the network size, is randomly set to be infected. Once a node becomes infected, it is given an exponentially distributed random time interval with mean $1/\alpha$, after which time it becomes recovered, and simultaneously it is assigned an exponentially distributed random time interval with mean $1/\gamma$, after which time it becomes treated. Once a node gets treated, it is given an exponentially distributed random time interval with mean $1/\eta$, after which time it becomes recovered. Once a node is infectious (infected or treated), contact events are generated along each edge emanating from this node. The time intervals for the contacts along each edge are exponentially distributed with mean $1/\tau$ and $1/(\delta\tau)$, respectively, depending on the node is infected or treated. If the node at the other end of an edge is susceptible, then it becomes infected at the time of contact; otherwise, nothing happens. The simulated process continues until it reaches a predetermined stop time, or there are no more infectious (infected or treated) nodes.

We generated a Poisson network with degree distribution $P(k) = \langle k \rangle^k e^{-\langle k \rangle} / k!$ ($\langle k \rangle = 6$) and a scale-free network with degree distribution $P(k) = C k^{-\nu}$ (C is a normalizing constant, $\nu = 2.1$ and $n = 80$). On each network, we conducted at least 100 independent stochastic simulations of the epidemic process, and compared the ensemble means of relevant variables with the outcomes of model (33) using the same network and disease parameters.

Figure 12 shows that, on a randomly generated Poisson network with $N = 6000$ and mean degree $\langle k \rangle = 6$, our model (33) agrees very well with the ensemble means of the stochastic simulations. The disease parameters are $\tau = 1.2$, $\delta = 0.1$, $\gamma = \alpha = 0.8$, and $\eta = 1$, resulting in $R_0 = 2.757 > 1$.

Figure 13 shows that, on a randomly generated scale-free network with $N = 6000$, exponent $\nu = 2.1$, minimum degree $k_{\min} = 3$, mean degree $\langle k \rangle = 8.24$ and vari-

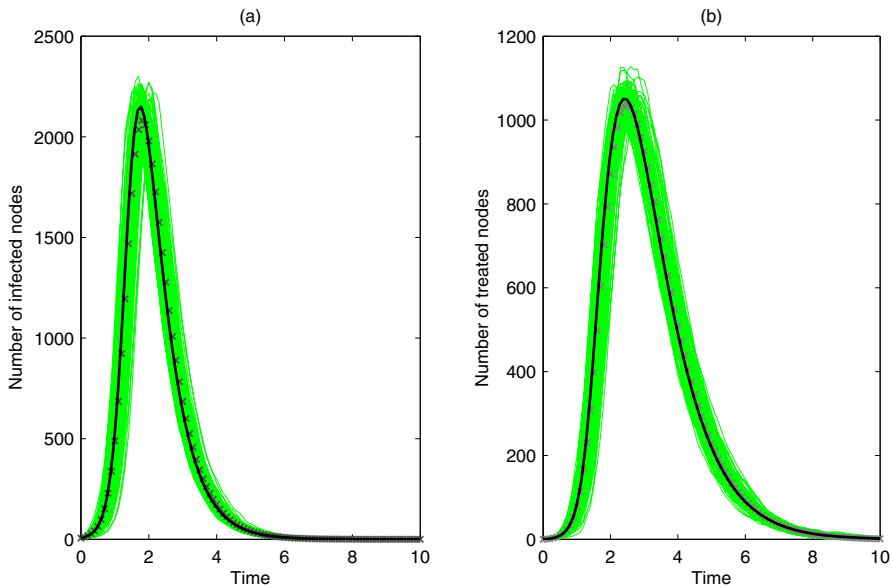


Fig. 12 Comparison of the outcomes (solid black lines) of our ODE model (33) with the ensemble means (gray crosses) of 100 stochastic simulations (thin green lines) on a Poisson network with $N = 6000$ and $\langle k \rangle = 6$. Disease parameters are: $\tau = 1.2$, $\delta = 0.1$, $\gamma = \alpha = 0.8$, and $\eta = 1$ (thus $R_0 = 2.757 > 1$). **a** Time evolution of the number of infected nodes; **b** Time evolution of the number of treated nodes (Color figure online)

ance $\text{Var}[k] = 95.49$, although our model outcomes cut through most simulation trajectories and behave similarly to the ensemble means, the ensemble means may not capture disease behavior accurately (e.g., the peak) due to stochastic fluctuations. In fact, we conducted 200 runs of stochastic simulations, out of which 18 runs lead to minor outbreaks (not present in the figure). To relieve this, one can use larger initial conditions or infection rate, or conduct a large number of stochastic simulations, say 500, ignoring the trajectories that the epidemic is not established in a network. The disease parameters are the same as in Fig. 12 except setting $\tau = 0.2515$ such that the basic reproduction number is the same as in Fig. 12. However, Fig. 14 shows that the ensemble mean is a good representation of the final size of the stochastic Sitr epidemic process, and the dotted black line denotes the theoretical prediction of the final size equation given in Sect. 3.3.

Figure 15 shows that increasing the infection rate on the same scale-free network as in Fig. 13, e.g., $\tau = 1.2$, our model (33) agrees very well with the ensemble means of the stochastic simulations.

3.3 Basic Reproduction Number and Final Epidemic Size

To calculate the basic reproduction number R_0 for model (33), we linearize the equations for ϕ'_I and ϕ'_T about the disease-free equilibrium ($\theta = 1$, $\phi_I = 0$ and $\phi_T = 0$)

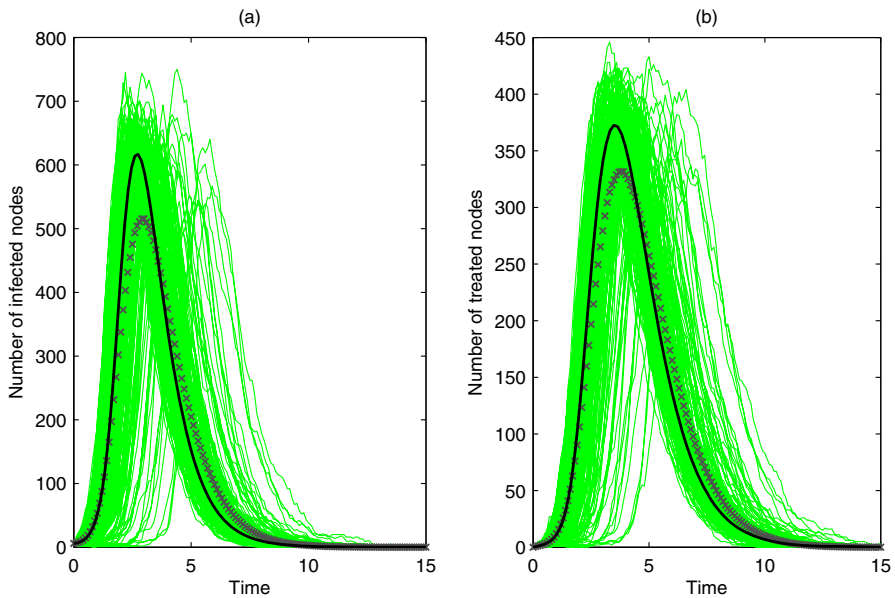


Fig. 13 Comparison of the outcomes (solid black lines) of our ODE model (33) with the ensemble means (gray crosses) of 182 stochastic simulations (thin green lines) on a scale-free network with $N = 6000$, exponent $\nu = 2.1$ and minimum degree $k_{\min} = 3$ (to avoid isolated pairs). Disease parameters are the same as in Fig. 12 except $\tau = 0.2515$ (such that $R_0 = 2.757$). **a** Time evolution of the number of infected nodes; **b** Time evolution of the number of treated nodes (Color figure online)

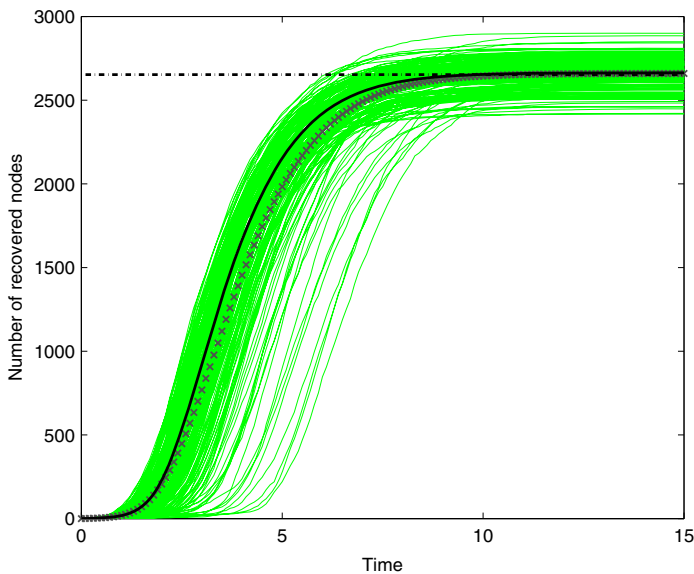


Fig. 14 Comparison of the outcome (solid black line) of our ODE model (33) with the ensemble mean (gray cross) of 182 stochastic simulations (thin green lines) on a scale-free network. The network and disease parameters are the same as in Fig. 13 (Color figure online)

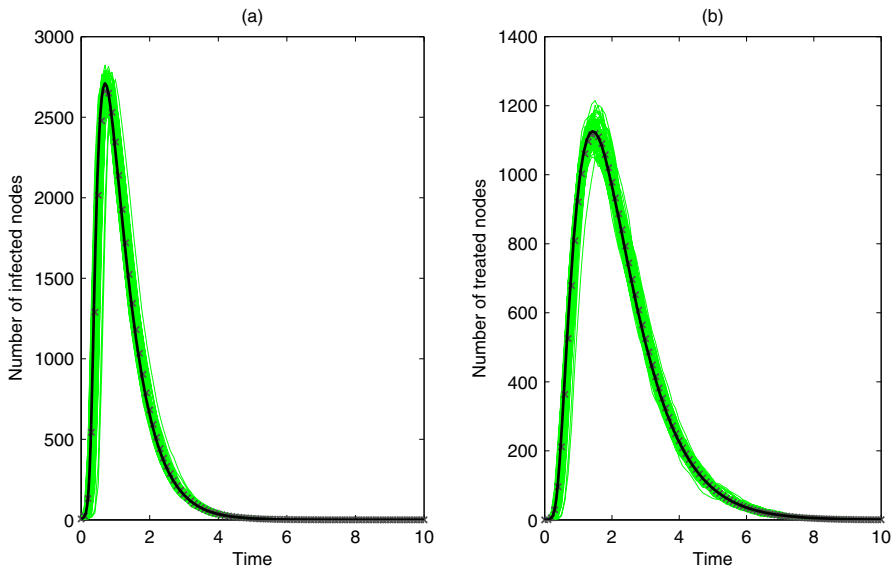


Fig. 15 Comparison of the outcomes (solid black lines) of our ODE model (33) with the ensemble means (gray crosses) of 100 stochastic simulations (thin green lines) on a scale-free network. The network parameters are the same as in Fig. 13, and the disease parameters are the same as in Fig. 12. **a** Time evolution of the number of infected nodes; **b** Time evolution of the number of treated nodes (Color figure online)

and get

$$\begin{cases} \phi_I' = \tau \frac{1}{\langle k \rangle} \sum_k k(k-1)P(k)(1-\epsilon_k)(\phi_I + \delta\phi_T) - (\tau + \alpha + \gamma)\phi_I, \\ \phi_T' = \gamma\phi_I - (\delta\tau + \eta)\phi_T. \end{cases} \quad (34)$$

Assuming $\epsilon_k \rightarrow 0$, $k = 1, 2, \dots$ and rewriting (34) in a matrix form yield

$$\frac{d}{dt} \begin{pmatrix} \phi_I \\ \phi_T \end{pmatrix} = (F_2 - V_2) \begin{pmatrix} \phi_I \\ \phi_T \end{pmatrix},$$

where

$$F_2 = \begin{bmatrix} \tau \frac{\langle k(k-1) \rangle}{\langle k \rangle} & \delta\tau \frac{\langle k(k-1) \rangle}{\langle k \rangle} \\ 0 & 0 \end{bmatrix} \text{ and } V_2 = \begin{bmatrix} \tau + \alpha + \gamma & 0 \\ -\gamma & \delta\tau + \eta \end{bmatrix}.$$

Then, it follows that

$$F_2 V_2^{-1} = \begin{bmatrix} \left(\frac{\tau}{\tau + \alpha + \gamma} + \frac{\gamma}{\tau + \alpha + \gamma} \frac{\delta\tau}{\delta\tau + \eta} \right) \frac{\langle k(k-1) \rangle}{\langle k \rangle} & \frac{\delta\tau}{\delta\tau + \eta} \frac{\langle k(k-1) \rangle}{\langle k \rangle} \\ 0 & 0 \end{bmatrix}.$$

Hence,

$$R_0 = \rho(F_2 V_2^{-1}) = \left(\frac{\tau}{\tau + \alpha + \gamma} + \frac{\gamma}{\tau + \alpha + \gamma} \frac{\delta\tau}{\delta\tau + \eta} \right) \frac{\langle k(k-1) \rangle}{\langle k \rangle},$$

where $\tau/(\tau + \alpha + \gamma)$ is the probability that a randomly chosen infected neighbor has transmitted infection before it becomes treated or recovered, $\gamma/(\tau + \alpha + \gamma)$ is the probability it becomes treated, $\delta\tau/(\delta\tau + \eta)$ is the probability that a randomly chosen treated neighbor has transmitted infection before it becomes recovered, and $\langle k(k-1) \rangle / \langle k \rangle$ is the average excess degree of a network.

To derive the final size equation, we look for $\theta(+\infty)$. Note that $d\theta/dt \leq 0$ and $0 \leq \theta \leq 1$. Thus, $\theta(+\infty)$ exists. Integrating the first equation of (33) from 0 to t gives

$$\theta(t) - 1 = -\tau \int_0^t \phi_I(s) ds - \delta\tau \int_0^t \phi_T(s) ds. \quad (35)$$

Observing that $\phi'_S + \phi'_I = -(\tau + \alpha + \gamma)\phi_I$, then integrating it from 0 to t yields

$$\phi_S(t) + \phi_I(t) - 1 = -(\tau + \alpha + \gamma) \int_0^t \phi_I(s) ds, \quad t > 0. \quad (36)$$

Similarly, observing that $\phi'_S + \phi'_I + \phi'_T = -(\tau + \alpha)\phi_I - (\delta\tau + \eta)\phi_T$, we have

$$\phi_S(t) + \phi_I(t) + \phi_T(t) - 1 = -(\tau + \alpha) \int_0^t \phi_I(s) ds - (\delta\tau + \eta) \int_0^t \phi_T(s) ds, \quad (37)$$

for any $t > 0$.

From Eq. (36), we obtain

$$\int_0^t \phi_I(s) ds = \frac{1}{\tau + \alpha + \gamma} - \frac{1}{\tau + \alpha + \gamma} (\phi_S(t) + \phi_I(t)). \quad (38)$$

Substituting Eq. (38) into Eq. (37), we obtain

$$\int_0^t \phi_T(s) ds = \frac{\gamma}{(\delta\tau + \eta)(\tau + \alpha + \gamma)} (1 - \phi_S(t) - \phi_I(t)) - \frac{1}{\delta\tau + \eta} \phi_T(t). \quad (39)$$

Substituting Eqs. (38) and (39) into Eq. (35) gives

$$\theta(t) - 1 = Q(\phi_S(t) + \phi_I(t) - 1) + \frac{\delta\tau}{\delta\tau + \eta} \phi_T(t), \quad (40)$$

where $Q = \frac{\tau}{\tau + \alpha + \gamma} + \frac{\gamma}{\tau + \alpha + \gamma} \frac{\delta\tau}{\delta\tau + \eta}$.

Letting $t \rightarrow +\infty$ and using $\phi_I(+\infty) = \phi_T(+\infty) = 0$, we have

$$\theta(+\infty) = 1 - Q \left(1 - \langle k \rangle^{-1} \sum_k k P(k) (1 - \epsilon_k) \theta^{k-1} (+\infty) \right). \quad (41)$$

Hence, the final size equation is given by

$$Z = R(+\infty) = 1 - S(+\infty) = 1 - \sum_k (1 - \epsilon_k) P(k) \theta^k(+\infty), \quad (42)$$

where $\theta(+\infty)$ can be solved from Eq. (41).

Let $J(y) = 1 - Q(1 - \langle k \rangle^{-1} \sum_k k P(k)(1 - \epsilon_k)y^{k-1})$, $y \in (0, 1]$. Next our goal is to show that the fixed point equation $y = J(y)$ has a unique solution $y^* \in (0, 1)$ for any $\epsilon_k \in (0, 1]$, $k = 1, \dots, n$. In the case when there are no infected individuals at the initial time, i.e., $\sum_k \epsilon_k = 0$, all individuals are susceptible, then we have the trivial solution $y_0 = 1$ and $R(+\infty) = 0$. The more interesting case is to consider the limit $R(+\infty)$ as $\sum_k \epsilon_k$ tends to zero. If the limit $R(+\infty)$ is zero then there is no epidemic with an infinitesimal initial infection. However, if the limit is positive, meaning that even an infinitesimal initial infection can cause a positive final epidemic size. Our derivation will also give the threshold condition separating the two regime. We have the following main result.

Theorem 3.1 Assume that $\tau + \alpha + \gamma > 0$ and $\delta\tau + \eta > 0$. Then, it holds that

- (a) $J(1) = 1$ (i.e., with 1 as a fixed point) if and only if $\epsilon_k = 0$, $k = 1, \dots, n$;
- (b) If $\sum_k \epsilon_k = 0$ and $R_0 > 1$, then there exists another unique fixed point of J in $(0, 1)$, whereas $R_0 \leq 1$ there exists the trivial fixed point only and $J(y) > y$ in $(0, 1)$;
- (c) If $\epsilon_k > 0$ for some $k = 1, \dots, n$, i.e., $\sum_k \epsilon_k > 0$, then it admits a unique fixed point y^* of J in $(0, 1)$, moreover, $J(y) > y$ in $(0, y^*)$ and $J(y) < y$ in $(y^*, 1)$.

Proof Direct calculation gives

$$J'(y) = Q\langle k \rangle^{-1} \sum_k k(k-1)P(k)(1 - \epsilon_k)y^{k-2} \geq 0, \quad J''(y) \geq 0,$$

meaning that J and J' are monotone increasing. In particular, if $\epsilon_k > 0$ for some $k = 1, \dots, n$, then J is strictly increasing and strictly convex in $(0, 1)$.

The proofs of (a), (b) and (c) are similar to those of Theorem 2.9, so we omit them here. \square

Remark 3.2 Using the method in Wang et al. (2018), model (33) can be easily extended to Sitr dynamics in degree-correlated quenched networks. Specifically, the probability that a node of degree k has not yet spread infection to a neighbor through its k edges should be θ_k . Then, the degree correlation (mixing pattern) influences the final size equations.

Remark 3.3 Alternatively, Eq. (41) can be obtained by considering the underlying stochastic process of an epidemic. Noting that Q is the probability that a randomly chosen neighbor has spread the infection provided that the neighbor becomes infected or treated, $\kappa_\infty = \langle k \rangle^{-1} \sum_k k P(k)(1 - \epsilon_k)\theta^{k-1}(+\infty)$ is the probability that the neighbor never becomes infected or treated (provided that the ego does not spread infection),

and $Q(1 - \kappa_\infty)$ is the probability of receiving infection from a neighbor, thus the probability that a neighbor of a randomly chosen edge does not acquire infection is

$$\theta(+\infty) = 1 - Q(1 - \kappa_\infty) = 1 - Q + Q\kappa_\infty,$$

which agrees with Eq. (41). If $P(k) = \langle k \rangle^k e^{-\langle k \rangle} / k!$ (Poisson degree distribution), $k = 0, 1, 2, \dots$, then $R_0 = Q\langle k \rangle$. In particular, if $\epsilon_k = 0$, $k = 1, \dots, n$, it follows that

$$\theta(+\infty) = 1 - Q + Qe^{-\langle k \rangle(1-\theta(+\infty))}.$$

Thus, the final size Eq. (42) reduces to

$$Z = 1 - e^{-\langle k \rangle(1-\theta(+\infty))} = 1 - e^{-Q\langle k \rangle Z} = 1 - e^{-R_0 Z},$$

consisting with the classical final size relation (Kermack and McKendrick 1927; Ma and Earn 2006). However, this classical final size relation does not hold for other degree distributions.

Remark 3.4 Theorem 3.1 (a) tells us that there will be no epidemic in the network if and only if there are no infectious seeds initially, corresponding to the disease-free equilibrium $\theta(+\infty) = 1$. However, if $\epsilon_k > 0$ for some $k = 1, \dots, n$, there will be an epidemic, and Theorem 3.1 (c) provides a numerical method to estimate the final epidemic size Z in degree uncorrelated quenched networks. Specifically, if $\epsilon_k > 0$ for some $k = 1, \dots, n$, i.e., $\sum_k \epsilon_k > 0$ or $\sum_k \epsilon_k = 0$ and $R_0 > 1$, there exists a unique fixed point $y^* \in (0, 1)$ of the function $J(y)$, and the sequence defined by the iteration $y_{j+1} = J(y_j)$ for any initial value $y_0 \in (0, 1)$ converges to y^* . The argument is similar to that in Remark 2.12, so it is omitted here.

In Fig. 16, we show the combined influence of network topology and treatment on the final epidemic size. Not surprisingly, the final epidemic size decreases with γ , and there exists a critical treatment rate γ^* , above which only small outbreaks occur. Moreover, network topology is a significant factor influencing the treatment of infected individuals.

4 Concluding Remarks

To investigate the potential influence of heterogeneous contacts and treatment on the spread and control of infectious diseases in a population, we have formulated epidemic models with partly effective treatment in annealed or quenched networks. The novelty of the model is that they include both contact heterogeneity and treatment of the infected individuals. For Sitr epidemic in annealed networks with degree correlation, we obtain the basic reproduction number, derive the implicit final size equations, and analyze the solvability of the solutions for these implicit equations. In particular, when there is no degree correlation in annealed networks, we derive a low-dimensional ODE

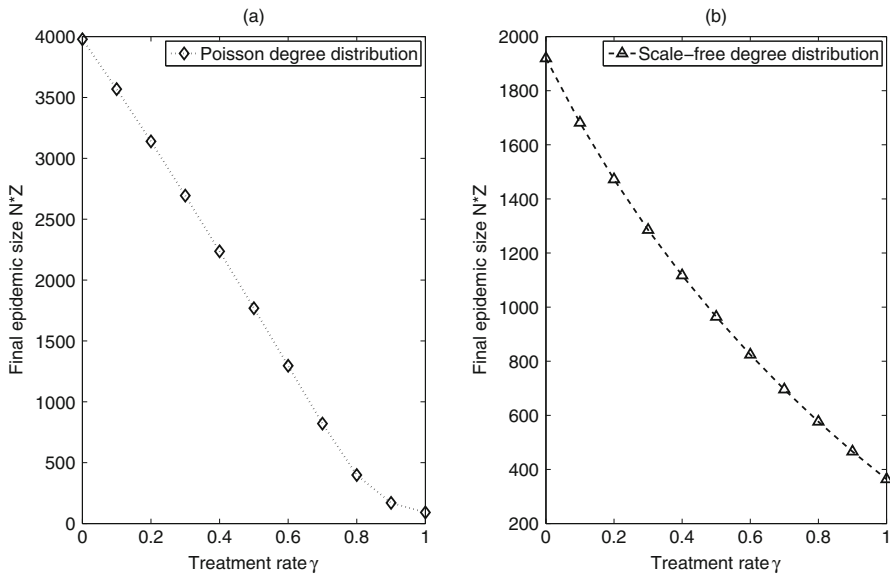


Fig. 16 The dependency of the final epidemic size for a Poisson and a scale-free networks on the treatment rate γ . **a** The network and other disease parameters are the same as in Fig. 12 except $\tau = 0.3$; **b** The network and other disease parameters are the same as in Fig. 13 except $\tau = 0.1$ (Online version in color)

system of Sitr epidemic dynamics, obtain the explicit expression of the basic reproduction number and a integrated final size equation, and discuss the solvability of this implicit final size equation. Moreover, for Sitr epidemic in quenched networks with no degree correlation, we derive a low-dimensional ODE system of Sitr epidemic dynamics, compare model outcomes with stochastic epidemic process, and obtain the basic reproduction number and a integrated final size equation. Furthermore, the solvability of implicit final size equation is considered.

The annealed network assumes that the network is constantly rewired while the quenched network assumes that the network is fixed. If the only available information about a population (network) is the number of contacts (degree distribution), one can use our low-dimensional ODE model (19) or (33) to estimate the peak size, the arrival time of the peak and the final epidemic size. In particular, the peak of treated individuals and the arrival time of the peak can be estimated numerically from our models, and we believe that these information can help the public health department to allocate medical resource reasonably and take necessary measures timely, especially when facing a new emerging disease like COVID-19.

It should be mentioned that there are some extensions in the following directions. First, the time scales for network dynamics and epidemic processes are comparable in a real-world population, thus contacts among individuals change as disease progresses, and edges disconnection or formation should be considered. Specifically, to obtain a low-dimensional co-evolution model of epidemics and network, we may need introducing a suitable time-varying probability generating function $g(x, t)$, which leads to a set of partial differential equations. Noting that the mean degree and the second

moment of a degree distribution is only related to the partial derivatives for dummy variable $x = 1$, this set of partial differential equations can be transformed to a set of ordinary differential equations, including equations for the time evolution of the moments of the degree distribution. Based on these new equations, we derive the basic reproduction number of the model; to obtain final epidemic size equations, we consider the limit system of the model (i.e., $t \rightarrow +\infty$) and introduce some suitable combinations of parameters like (Keeling et al. 1997).

Second, our model considers only the case that resources for treatment are quite large, that is, the treatment for infected individuals is assumed to be proportional to the number or fraction of infected individuals. However, for a community with limited capacity for treatment, a constant treatment (Wang and Ruan 2004) or treatment with saturation effect (Wang 2006) is more suitable. Thirdly, the data on COVID-19 are gathered by WHO in most countries or regions and are available, we would like to validate our model with the real data. Last but not least, nodes and edges of complex networks are embedded in space, so space is a relevant factor influencing population or epidemic dynamics (Sun et al. 2017, 2018; Guo et al. 2019). We leave these interesting extensions of our model for future work.

Acknowledgements This research is partially supported by (i) National Natural Science Foundation of China under Grants 12171443, 12271314 and 11801532, and Key Project of Natural Science Foundation of China under Grant 61833005, (ii) Fundamental Research Funds for the Central Universities, China University of Geosciences (Wuhan) under Grant CUGSX01, (iii) China Postdoctoral Science Foundation under Grants 2019T120372 and 2018M630490.

References

- Anderson RM, Anderson B, May RM (1992) Infectious diseases of humans: dynamics and control. Oxford University Press, Oxford
- Arino J, Brauer F, van den Driessche P, Watmough J, Wu J (2007) A final size relation for epidemic models. *Math Biosci Eng* 4:159–175
- Bac  r N, Guernaoui S (2006) The epidemic threshold of vector-borne diseases with seasonality. *J Math Biol* 53:421–436
- Barab  si AL, Albert R (1999) Emergence of scaling in random networks. *Science* 286:509–512
- Berman A, Plemmons RJ (1994) Nonnegative matrices in the mathematical sciences. SIAM, Philadelphia
- Bidari S, Chen X, Peters D, Pittman D, Simon PL (2016) Solvability of implicit final size equations for SIR epidemic models. *Math Biosci* 282:181–190
- Brauer F (2008) Epidemic models with heterogeneous mixing and treatment. *Bull Math Biol* 70:1869–1885
- Brauer F (2017) A final size relation for epidemic models of vector-transmitted diseases. *Infect Dis Model* 2:12–20
- Brauer F, Castillo-Chavez C (2012) Mathematical models in population biology and epidemiology. Springer, New York
- Cao J, Wang Y et al (2015) Global stability of an epidemic model with carrier state in heterogeneous networks. *IMA J Appl Math* 80:1025–1048
- Corcoran C, Hastings A (2021) A low-dimensional network model for an SIS epidemic: analysis of the super compact pairwise model. *Bull Math Biol* 83:1–26
- Diekmann O, Heesterbeek JAP, Metz JAJ (1990) On the definition and the computation of the basic reproduction ratio R_0 in models for infectious diseases in heterogeneous populations. *J Math Biol* 28:365–382
- Diekmann O, Heesterbeek JAP, Roberts MG (2010) The construction of next-generation matrices for compartmental epidemic models. *J R Soc Interface* 7:873–885
- Eames KTD, Keeling MJ (2002) Modeling dynamic and network heterogeneities in the spread of sexually transmitted diseases. *Proc Natl Acad Sci USA* 99:13330–13335

- Feng ZL, Castillo-Chavez C, Capurrode F (2000) A model for tuberculosis with exogenous reinfection. *Theor Pop Biol* 57:235–247
- Gillespie DT (1976) A general method for numerically simulating the stochastic time evolution of coupled chemical reactions. *J Comput Phys* 22:403–434
- Guo Z-G, Song L-P, Sun G-Q, Li C, Jin Z (2019) Pattern dynamics of an SIS epidemic model with nonlocal delay. *Int J Bifurcat Chaos* 29:1950027
- Gupta C, Tuncer N, Martcheva M (2021) A network immuno-epidemiological HIV model. *Bull Math Biol* 83:1–29
- Hethcote HW (2000) The mathematics of infectious diseases. *SIAM Rev* 42:599–653
- Keeling MJ (1999) The effects of local spatial structure on epidemiological invasions. *Proc R Soc Lond B* 266:859–867
- Keeling MJ, Rohani P (2011) Modeling infectious diseases in humans and animals. Princeton University Press, Princeton
- Keeling MJ, Rand DA, Morris AJ (1997) Correlation models for childhood epidemics. *Proc R Soc Lond B* 264:1149–1156
- Kermack WO, McKendrick AG (1927) A contribution to the mathematical theory of epidemics. *Proc R Soc Lond Ser A* 115:700–721
- Kiss IZ, Green DM, Kao RR (2006) The effect of contact heterogeneity and multiple routes of transmission on final epidemic size. *Math Biosci* 203:124–136
- Levin SA, Durrett R (1996) From individuals to epidemics. *Phil Trans R Soc Lond B* 351:1615–1621
- Lindquist J, Ma JL, Driessche P, Willeboordse FH (2011) Effective degree network disease models. *J Math Biol* 62:143–164
- Ma JL, Earn DJD (2006) Generality of the final size formula for an epidemic of a newly invading infectious disease. *Bull Math Biol* 68:679–702
- Magal P, Webb G (2018) The parameter identification problem for SIR epidemic models: identifying unreported cases. *J Math Biol* 77:1629–1648
- Magal P, Seydi O, Webb G (2016) Final size of an epidemic for a two-group SIR model. *SIAM J Appl Math* 76:2042–2059
- Magal P, Seydi O, Webb G (2018) Final size of a multi-group SIR epidemic model: irreducible and non-irreducible modes of transmission. *Math Biosci* 301:59–67
- Mieghem PV, Omic J, Kooij R (2009) Virus spread in networks. *IEEE/ACM Trans Netw* 17:1–14
- Miller JC, Slim AC, Volz E (2012) Edge-based compartmental modelling for infectious disease spread. *J R Soc Interface* 9:890–906
- Molloy M, Reed B (1995) A critical point for random graphs with a given degree sequence. *Random Struct Algorithms* 6:161–179
- Moreno Y, Pastor-Satorras R, Vespignani A (2002) Epidemic outbreaks in complex heterogeneous networks. *Eur Phys J B* 26:521–529
- Newman MEJ (2002) Spread of epidemic disease on networks. *Phys Rev E* 66:016128
- Newman MEJ (2010) Networks: an introduction. Oxford University Press, New York
- Paré PE, Beck CL, Başar T (2020) Modeling, estimation, and analysis of epidemics over networks: an overview. *Annu Rev Control* 50:345–360
- Pastor-Satorras R, Vespignani A (2001) Epidemic spreading in scale-free networks. *Phys Rev Lett* 86:3200–3203
- Pastor-Satorras R, Vespignani A (2002) Epidemic dynamics in finite size scale-free networks. *Phys Rev E* 65:035108(R)
- Pastor-Satorras R, Castellano C, Mieghem P, Vespignani A (2015) Epidemic processes in complex networks. *Rev Mod Phys* 87:925–979
- Sanz J, Xia CY, Meloni S, Moreno Y (2014) Dynamics of interacting diseases. *Phys Rev X* 4:041005
- Sun G-Q, Jusup M, Jin Z, Wang Y, Wang Z (2016) Pattern transitions in spatial epidemics: mechanisms and emergent properties. *Phys Life Rev* 19:43–73
- Sun G-Q, Wang C-H, Wu Z-Y (2017) Pattern dynamics of a Gierer–Meinhardt model with spatial effects. *Nonlinear Dynam* 88:1385–1396
- Sun G-Q, Wang C-H, Chang L-L, Wu Y-P, Li L, Jin Z (2018) Effects of feedback regulation on vegetation patterns in semi-arid environments. *Appl Math Model* 61:200–215
- van den Driessche P, Watmough J (2002) Reproduction numbers and sub-threshold endemic equilibria for compartmental models of disease transmission. *Math Biosci* 180:29–48
- Volz E (2008) SIR dynamics in random networks with heterogeneous connectivity. *J Math Biol* 56:293–310

- Wang WD (2006) Backward bifurcation of an epidemic model with treatment. *Math Biosci* 201:58–71
- Wang Y, Cao JD (2014) Global dynamics of a network epidemic model for waterborne diseases spread. *Appl Math Comput* 237:474–488
- Wang Y, Cao J (2021) Final size of network epidemic models: properties and connections. *Sci China Inf Sci* 64:179201
- Wang L, Dai GZ (2008) Global stability of virus spreading in complex heterogeneous networks. *SIAM J Appl Math* 68:1495–1502
- Wang W, Ruan S (2004) Bifurcation in an epidemic model with constant removal rate of the infectives. *J Math Anal Appl* 291:775–793
- Wang W, Zhao XQ (2008) Threshold dynamics for compartmental epidemic models in periodic environments. *J Dyn Diff Equat* 20:699–717
- Wang Y, Jin Z, Yang ZM, Zhang ZK, Zhou T, Sun GQ (2012) Global analysis of an SIS model with an infective vector on complex networks. *Nonlinear Anal RWA* 13:543–557
- Wang Y, Ma JL, Cao JD, Li L (2018) Edge based epidemic spreading in degree-correlated complex networks. *J Theor Biol* 454:164–181
- World Health Organization (April 2022) Weekly epidemiological update on COVID-19 - 27. <https://www.who.int/publications/m/item/weekly-epidemiological-update-on-covid-19--27-april-2022>
- Yan C, Wang W (2019) Modeling HIV dynamics under combination therapy with inducers and antibodies. *Bull Math Biol* 81:2625–2648
- Zhang J, Jin Z (2010) The analysis of epidemic network model with infectious force in latent and infected period. *Discret Dyn Nat Soc* 2010:604329
- Zhang J, Jin Z (2012) Epidemic spreading on complex networks with community structure. *Appl Math Comput* 219:2829–2838
- Zhang J, Li D, Jing W, Jin Z, Zhu H (2019) Transmission dynamics of a two-strain pairwise model with infection age. *Appl Math Model* 71:656–672
- Zino L, Cao M (2021) Analysis, prediction, and control of epidemics: a survey from scalar to dynamic network models. *IEEE Circ Syst Mag* 21:4–23

Publisher's Note Springer Nature remains neutral with regard to jurisdictional claims in published maps and institutional affiliations.

Springer Nature or its licensor (e.g. a society or other partner) holds exclusive rights to this article under a publishing agreement with the author(s) or other rightsholder(s); author self-archiving of the accepted manuscript version of this article is solely governed by the terms of such publishing agreement and applicable law.